



1 **Tree-grass phenology information improves light use** 2 **efficiency modelling of gross primary productivity for an** 3 **Australian tropical savanna**

4
5 Caitlin E Moore¹, Jason Beringer^{1,2}, Bradley Evans^{3,4}, Lindsay B Hutley⁵, Nigel J Tapper¹

6 ¹ School of Earth, Atmosphere and Environment, Monash University, Clayton, VIC, 3800, Australia

7 ² School of Earth and Environment, The University of Western Australia, Crawley, WA, 6009, Australia

8 ³ Department of Environmental Sciences, The University of Sydney, Eveleigh, NSW, 2015, Australia

9 ⁴ Terrestrial Ecosystem Research Network Ecosystem Modelling and Scaling Infrastructure, The University of
10 Sydney, Eveleigh, NSW, 2015, Australia

11 ⁵ School of Environment, Research Institute for the Environment and Livelihoods, Charles Darwin University,
12 Casuarina, NT, 0909, Australia

13 *Correspondence to:* Caitlin E Moore (caitlin@moorescience.com.au)

15 **Abstract**

16 The coexistence of trees and grasses in savanna ecosystems results in marked phenological dynamics
17 that vary spatially and temporally with climate. Australian savannas comprise a complex variety of
18 life forms and phenologies, from evergreen trees to annual/perennial grasses, producing a boom-bust
19 seasonal pattern of productivity that follows the wet-dry seasonal rainfall cycle. As the climate
20 changes into the 21st Century, modification to rainfall and temperature regimes in savannas is highly
21 likely. There is a need to link phenology cycles of different species with productivity to understand
22 how the tree-grass relationship may shift in response to climate change. This study investigated the
23 relationship between productivity and phenology for trees and grasses in an Australian tropical
24 savanna. Productivity, estimated from overstory (tree) and understory (grass) eddy covariance flux
25 tower estimates of gross primary productivity (GPP), was compared against two years of repeat time-
26 lapse digital photography (phenocams). We explored the phenology-productivity relationship at the
27 ecosystem scale using moderate resolution imaging spectroradiometer (MODIS) vegetation indices
28 and flux tower GPP. These data were obtained from the Howard Springs OzFlux/Fluxnet site (AU-
29 How) in northern Australia. Two greenness indices were calculated from the phenocam images; the
30 green chromatic coordinate (GCC) and excess green index (ExG). These indices captured the
31 temporal dynamics of the understory (grass) and overstory (trees) phenology, and were mostly well
32 correlated with tower GPP for understory ($r^2 = 0.65$ to 0.72) and overstory ($r^2 = 0.09$ to 0.23). The
33 MODIS enhanced vegetation index (EVI) correlated well with GPP at the ecosystem scale ($r^2 = 0.70$).



1 Lastly, we used GCC and EVI to parameterise a light use efficiency (LUE) model and found it to
2 improve the estimates of GPP for the overstory, understory and ecosystem. We conclude that
3 phenology is an important parameter to consider in estimating GPP from LUE models in savannas and
4 that phenocams can provide important insights into the phenological variability of trees and grasses.

5 **Key Words**

6 Eddy covariance, phenocam, leaf area index, photosynthetically active radiation, light use efficiency,
7 MODIS, OzFlux

8 **1 Introduction**

9 Savanna ecosystems are defined by the coexistence of trees and grasses, and have evolved to
10 dominate one fifth of the terrestrial land surface (Scholes and Archer, 1997; Grace et al., 2006). In
11 tropical savanna, trees utilise the C_3 photosynthetic pathway, whereas the grasses use the more
12 recently evolved C_4 pathway, being more efficient at taking up carbon in hot environments with
13 limited water and nutrient availability (Sage, 2004; Osborne and Beerling, 2006). Savannas are
14 typically found in wet/dry climates that over time have shaped the tree-grass structure and phenology
15 seen today. Fire also plays a role in shaping savanna phenology and structure, with recurrences often
16 every 1-5 years (Hoffmann et al., 2012; Beringer et al., 2015), fire consumes cured grass biomass in
17 the dry season and suppresses growth of juvenile overstory species, resulting in a range of plant
18 phenology responses to deal with it (Bond, 2008; Murphy et al., 2010; Werner and Franklin, 2010).
19 Herbivory, drought and land-use change are additional disturbances that commonly occur in savannas
20 (Hutley and Beringer, 2011). These complex interactions are believed to be the primary reason for the
21 co-dominance of trees and grasses in savanna ecosystems, as well as for the phenological variability
22 displayed (Bond et al., 2003; Van Langevelde et al., 2003; Bond, 2008; Hanan and Lehmann,
23 2010; Lehmann et al., 2014).

24 The climate and disturbance regime in savannas plays an important role in shaping plant phenology.
25 C_4 savanna grasses typically follow a boom-bust phenological cycle, where they rapidly produce
26 biomass in the wet season and display an annual or perennial die-back phenology in the dry season
27 (Bond, 2008; Ratnam et al., 2011). C_3 savanna trees, in contrast, can range from having a fully
28 deciduous phenology to remaining evergreen throughout the dry season. In Australian savannas, the
29 understory is dominated by C_4 annual grasses with a small portion represented by juvenile overstory
30 species (Werner and Franklin, 2010; Werner and Prior, 2013) and perennial grasses. Evergreen
31 eucalypt species make up the bulk (~ 80 %) of the overstory in Australian savannas (Hutley et al.,
32 2011), however, semi-, brevi- and fully deciduous species are found to a lesser degree throughout
33 (Williams et al., 1997) and contribute to the seasonal fluctuation of canopy leaf area (O'Grady et al.,
34 2000; Whitley et al., 2011). Tree-grass ratios are driven by annual rainfall, and in Australia there is a



1 strong rainfall gradient from the coast inland (Rogers and Beringer, 2016), resulting in northern high
2 rainfall (mesic) regions supporting higher tree-grass ratios and drier southern (xeric) regions
3 supporting higher grass-tree ratios (Hutley et al., 2011;Ma et al., 2013).

4 The monitoring of savanna phenology can inform how savannas might respond to climate change. At
5 the regional scale, the timing of phenological events varies widely for savannas due to variability in
6 the occurrence and duration of rainfall events (Ma et al., 2013). Phenology, in turn, influences the
7 productivity and growth (carbon cycle) of an ecosystem, as well as its water and nutrient cycles
8 (Noormets, 2009;Richardson et al., 2013). The savanna region of Australia is projected to experience
9 warming and increased rainfall (variability and amount) under climate change (Reisinger et al., 2014),
10 which is likely to impact savanna phenology and its interactions with the carbon, nutrient and water
11 cycles (Kanniah et al., 2010;Scheiter et al., 2015). There is a need for better understanding of what
12 governs savanna phenology in order to predict how it may be affected by climate change (Beringer et
13 al., 2016a).

14 Due to the large extent and spatial variation of savannas, satellite remote sensing provides a useful
15 tool (Broich et al., 2015) for examining the interactions of savanna phenology with productivity.
16 Vegetation indices such as the normalised difference vegetation index (NDVI) (Tucker, 1979) and
17 enhanced vegetation index (EVI) (Huete et al., 2002) provide valuable measures of savanna
18 phenological variability from the landscape to global scale (Ma et al., 2013;Ma et al., 2014). Likewise,
19 the MODIS gross primary productivity (GPP) product (MOD17 A2/A3, Running and Zhao, 2015)
20 offers the most reliable means of estimating large scale savanna productivity (Grace et al., 2006;Ryu
21 et al., 2011), but has been shown to underestimate savanna GPP, particularly during the transition
22 between the wet and dry seasons (Kanniah et al., 2009;Whitley et al., 2011;Ma et al., 2014). Core
23 issues surrounding the remoteness of satellite sensors, the effects of cloud contamination on daily data
24 collection, the diffuse nature of light and the need to aggregate imagery spatially and temporally for
25 contiguous scenes, results in coarse temporal resolution (i.e. 8 or 16 day) satellite data products that
26 can be problematic for identifying change in seasonally cloudy tropical environments (Eberhardt et al.,
27 2016) where rapid (i.e. 1-2 weeks) phenological change is common (Williams et al., 1997;Moore et
28 al., 2016b).

29 A novel approach to alleviate some of the limitations of satellite remote sensing is to use *in situ*
30 automated time-lapse cameras (phenocams) that can collect high temporal resolution (hourly to daily)
31 images of vegetation within and above an ecosystem (Richardson et al., 2007;Hufkens et al.,
32 2012;Sonnentag et al., 2012;Moore et al., 2016b). The proximity of these cameras to ecosystem
33 vegetation allows them to capture important information about vegetation cover change via leaf
34 emergence and senescence (Richardson et al., 2007;Richardson et al., 2009a;Keenan et al., 2014) that
35 can be linked with measures of ecosystem GPP (Tans et al., 1990;Richardson et al., 2010;Toomey et



al., 2015). Phenocam data have also been used for parameterising light use efficiency (LUE) models (in a similar way to MODIS GPP) that describe ecosystem GPP through the relationship of absorbed photosynthetically active radiation (APAR) with that of plant LUE (Migliavacca et al., 2011).

In this study, we aim to contribute a detailed assessment of phenological cover change, and its relationship with productivity, for a mesic tropical savanna in northern Australia over 2 years. Our objectives are to (i) determine the utility of phenocams for identifying change in overstory and understory vegetation greenness; (ii) quantify the relationship between savanna overstory and understory phenology and productivity on seasonal and annual timescales; (iii) test if phenocam indices can be used as a proxy for improvement of a LUE model that is widely used to estimate GPP; and (iv) test the applicability of MODIS EVI for improving estimates of ecosystem scale GPP. To do this we utilise one of the first phenocam datasets obtained in Australian ecosystems, along with MODIS EVI, and couple them with previously collected ecosystem, overstory and understory eddy covariance data (Moore et al., 2016a) to tease apart the tree and grass phenology-productivity relationship in Australian savanna.

2 Methods

To address each of our objectives, we used a combination of eddy covariance and phenocam imagery along with information about overstory leaf area index (LAI), understory biomass and the radiation use of the overstory, understory and ecosystem over time. These data were used to tease apart the relationship between productivity and phenology for the trees (overstory) and grass (understory) so we could identify how they varied throughout the 2 year study period. Phenocam greenness phenology information and MODIS EVI were also used to parameterise a LUE model that we then used to estimate overstory, understory and ecosystem GPP.

2.1 Site Description

This study was conducted at the Howard Springs OzFlux (www.ozflux.org.au/) and Fluxnet (AU-How) site (Beringer et al., 2016a) near Darwin in the Northern Territory, Australia. A record of carbon, water and energy flux, as well as meteorological and soil measurements, was first established at Howard Springs in 1997 (Eamus et al., 2001). As such, many detailed site descriptions exist (Beringer et al., 2007; Hutley et al., 2013; Beringer et al., 2015; Moore et al., 2016a) so only a brief description is provided here. Annual rainfall for the Howard Springs area is 1732 mm (± 44 SE) mm, (Australian Bureau of Meteorology (BoM), station ID: 014015, www.bom.gov.au) of which 90-95 % falls within the rainy (wet) season months of October to April. For this study, we defined the wet season as a 6 month period from October 15th through to April 15th and the dry season as April 16th to October 14th based on the work of Cook and Heerdegen (2001). Mean daily maximum air temperature varies annually between 30.6 to 33.3 °C and mean daily minimum air temperature ranges from 19.3 to



1 25.3 °C (Australian Bureau of Meteorology, www.bom.gov.au/). Howard Springs is defined as a
2 mesic savanna because it receives >1200 mm rainfall annually (Hutley et al., 2011) and is classified
3 as ‘open forest savanna’ based on its canopy cover fraction (50–60 %) after Specht (1972). Soils are
4 mostly red Kandosols (Isbell, 1996) that are sandy-loamy, well weathered and nutrient poor.

5 Vegetation consists of a C₃ woody overstory that is dominated by evergreen *Eucalyptus miniata*
6 (Darwin woollybutt) and *E. tetradonta* (Darwin stringybark). A smaller portion of the tree canopy and
7 mid-canopy layer is made up of semi-, brevi- and fully deciduous species such as *Erythrophleum*
8 *chlorostachys* (Ironwood) and *Terminalia ferdinandiana* (Kakadu plum) (Williams et al., 1997; Hutley
9 et al., 2011). Mean canopy height is 18 m (Hutley et al., 2011). The understory is dominated by the
10 annual C₄ grass *Sorghum intrans* (spear grass) and perennial C₄ grasses *Heteropogon triticeous* and *S.*
11 *plumosum*. Also sharing the understory with the grasses are saplings (juveniles) of overstory species,
12 the shrub *Buchanania obovata* and the cycad *Cycas armstrongii*. Due to the frequent occurrence of
13 fire in Australian savanna (Beringer et al., 2015), control burning was performed at the beginning of
14 each dry season to protect the monitoring equipment at the Howard Springs flux site.

15 2.2 Productivity measurements

16 To estimate productivity from the savanna ecosystem and partition it into tree (overstory) and grass
17 (understory) GPP, we used the eddy covariance technique (Baldocchi et al., 2001) as detailed for
18 Howard Springs by Moore et al. (2016a). Two eddy covariance towers were in operation at Howard
19 Springs to measure the fluxes of carbon, water and energy from both the understory (within tree
20 canopy tower at 5 m) and the ecosystem (above tree canopy tower at 23 m). The overstory flux
21 component is simply the difference between ecosystem and understory fluxes and represents the
22 above ground tree fluxes. Instrumentation, validation of the understory tower, data quality assurance
23 and quality control (QA/QC) and flux partitioning information is also provided in Moore et al.
24 (2016a). Therefore, we provide only a brief description of the site instrumentation and flux data
25 processing.

26 Core eddy covariance instruments on each tower consisted of a 3D sonic anemometer (CSAT3,
27 Campbell Scientific, Logan UT) and an infra-red gas analyser (LI-7500, Li-COR Biosciences, Lincoln,
28 NE). These instruments sampled at a rate of 10 Hz and provided 30-min flux averages. Soil heat flux
29 (HFT3, Campbell Scientific, Logan, UT) and net/short/long wave radiation components were also
30 recorded on the ecosystem tower (CNR4, Kipp and Zonen, Delft, NL). The raw 30-minute data were
31 QA/QC'd to level 3 standard using the OzFluxQC (v2.9.4) python scripts. Energy balance closure
32 analysis of the ecosystem tower, based on daily data (Leuning et al., 2012), gave a slope of 0.89 and
33 an r^2 of 0.92. The understory tower was validated via power spectra analysis (Moore et al., 2016a) that
34 followed idealised curves for vegetated canopies (Kaimal and Finnigan, 1994). Level 3 data were then
35 gap filled and used to partition net ecosystem exchange (NEE) into respiration and GPP using the



1 Dynamic INtegrated Gap filling and partitioning for OzFlux (DINGO, (Beringer et al., 2016b))
2 package. Both OzFlux and DINGO packages were written using python scripts.

3 **2.3 Phenology and light use efficiency (LUE) measurements**

4 Alongside the flux tower estimates of tree and grass productivity, we recorded time series of incident,
5 reflected and absorbed PAR, as well as vegetation cover change. While the understory is largely
6 homogenous in species distribution at the flux tower footprint scale (i.e. >50 m), variation from one
7 point to the next does exist in the understory due to its vegetation composition. To obtain a rigorous
8 time series, spatial replicate measurements of vegetation cover change and PAR variability are
9 required. We used five towers (mini towers), each of which were 5 m tall and made from steel square
10 hollow section with a cross arm to attach the instruments and a logger-solar panel array. The towers
11 were stabilised using guy wires and a base plate. A winch system was used to manoeuvre the
12 instruments up and down the tower for data download and maintenance. The towers were set up at a
13 distance of 50 m in a pentagon shape around the main ecosystem flux tower and faced an east-west
14 direction (Fig. 1).

15 To measure the components of PAR in the savanna, we installed PAR sensors on each of the mini
16 towers (SQ-Series, Apogee, Logan, UT). Incoming PAR reaching the understory, through the
17 overstory vegetation, was measured with a PAR sensor installed facing upward at 5 m on each mini
18 tower. Another sensor was installed facing downward at 5 m to record the amount of PAR reflected
19 by the understory vegetation. The amount of PAR reaching the ground surface through the understory
20 vegetation was recorded with a third PAR sensor facing upward at 10 cm. A data logger (CR800,
21 Campbell Scientific, Logan UT) and multiplexor (AM25T, Campbell Scientific, Logan, UT) were
22 used to collect and store PAR data and to operate the phenocams. The mini tower system was
23 powered using a 20 W solar panel, 12 V regulator and 12 V gel cell battery. To provide a complete
24 accounting of PAR in the savanna, two additional PAR sensors (LI-190 Quantum Series, Li-COR
25 Biosciences, Lincoln, NE) were installed on the 23 m flux tower for collection of incoming PAR and
26 outgoing PAR reflected from the savanna ecosystem.

27 Changes in savanna overstory and understory vegetation greenness were assessed using consumer-
28 grade point-and-shoot cameras (Canon Powershot A810). Each mini tower supported two cameras,
29 one to collect upward facing images of the tree canopy and one to collect downward facing images of
30 the understory, making a total of 10 cameras installed. The cameras were set to run using automatic
31 exposure in aperture priority mode, with a low f/stop value of 2.8 to ensure the entire image was used
32 to respond to ambient light levels (Richardson et al., 2007; Ryu et al., 2012; Sonnentag et al., 2012).
33 Automatic white balance was also used as we did not have a grey reference panel to correct for white
34 balance manually. Images were stored on SD memory cards in a compressed JPEG file format, to
35 ensure the cards did not fill between site visits.



1 Each camera was housed in a waterproof case with an aperture hole cut in the top that was sealed with
2 a microscope slide (Fig. 2, a & d). Following the concept of Ryu et al. (2012), power was delivered to
3 the cameras through wires soldered to the battery terminals, which received input from a 12 V relay
4 connected with a 3.3 V regulator. A second 5 V relay was used to send a short pulse to wires soldered
5 onto the 'on-button' of the cameras to mimic the action of turning the cameras on. The Canon Hack
6 Development Kit (<http://chdk.wikia.com/wiki/CHDK>) was used to modify the cameras to
7 automatically take an image when turned on, which was administered via a u-Basic script saved on
8 the memory card. Each mini tower logger was programmed to operate the cameras twice daily, once
9 at 11:30 ACST (to match the MODIS Terra overpass) and once at 13:00 ACST (approximately solar
10 noon). Each camera was installed on the mini towers using a metal plate angled at 57.5 ° from zenith,
11 as this angle has been found to minimise the effects of leaf inclination angle when calculating LAI
12 (Weiss et al., 2004; Baret et al., 2010).

13 **2.4 Phenocam image and radiation data processing**

14 Phenocam images were firstly visually checked for field of view (FOV) shifts and major obstructions
15 (i.e. water on the case windows) as a first step in the image QA/QC process. Images with obstructions
16 were removed, which accounted for between 3 - 13 % of images for each camera. However, three out
17 of ten cameras were completely omitted from analysis due to severe FOV shifts or where an
18 individual camera had greater than 50% of images lost. This left a total of four cameras for understory
19 analysis (5031 images total) and three for the overstory (4255 images total). All remaining cameras (n
20 = 7) experienced slight FOV shifts as a result of manual data download. However, a Student t-test of
21 686 analysed images, for a camera with a large visible FOV shift, revealed no significant effect on the
22 extracted results ($t_{686} = 0.13$, $p = 0.90$). The time series from each camera were then gap filled using
23 the best regression relationship against another camera, most of which had an $r^2 > 0.8$.

24 For each camera, the images were analysed using code written in python that initially took the
25 extracted Exif (Exchangeable image file format) data to rename files using a standardised (yyyy-mm-
26 dd hh:mm:ss) format. Images were analysed in date/time succession using a region of interest (ROI)
27 that encompassed as much of the vegetation as feasible. As a result, the ROI varied depending on the
28 vegetation available in the overstory FOV and was the same for all understory cameras, except for a
29 separate analysis of grass and woody green vegetation, which required individual ROI's for each
30 understory camera (Fig. 2).

31 Each camera collected 8-bit depth red-green-blue (RGB) colour channel information, stored as digital
32 numbers (DN), at a resolution of 4608 x 3456 pixels. These DN's provide a measure of colour
33 intensity based on irradiance, so they can be highly variable when scene illumination changes (Ide and
34 Oguma, 2010; Sonnentag et al., 2012). To reduce the effects of scene illumination, the DN's are



1 typically used to calculate the green (GCC) chromatic coordinate, a normalised ratio of the green
2 channel to all channels, as Eq. (1) (Gillespie et al., 1987; Woebbecke et al., 1995):

$$3 \quad G_{cc} = G_{DN} / (R_{DN} + G_{DN} + B_{DN}) \quad (1)$$

4 where DN is the digital number that corresponds with the green (G), red (R) and blue (B) channels.
5 The red (RCC) and blue (BCC) chromatic coordinates were calculated in the same way as GCC.
6 Chromatic coordinate values were calculated for each pixel within the ROI and then averaged to give
7 an overall GCC, RCC and BCC value for each image. In addition to the chromatic coordinates, we
8 also calculated the excess green (ExG), red (ExR) and blue (ExB) indices in order to compare which
9 colour index performed best in capturing savanna phenological change. The excess index is an
10 enhancement of the respective colour channel information against the other channels and is calculated
11 as Eq. (2) (Woebbecke et al., 1995):

$$12 \quad ExG = 2G_{DN} - (R_{DN} + B_{DN}) \quad (2)$$

13 The amount of light used by vegetation over time is directly correlated with productivity (Monteith,
14 1972). Using the PAR data collected from the mini towers, we calculated fPAR for the overstory (OS)
15 Eq. (3), understory (US) Eq. (4) and ecosystem (ECO) Eq. (5) as:

$$16 \quad fPAR_{OS} = (PAR_{AED} - PAR_{AGD}) / PAR_{AED} \quad (3)$$

$$17 \quad fPAR_{US} = (PAR_{AGD} - PAR_{BGD}) / PAR_{AGD} \quad (4)$$

$$18 \quad fPAR_{ECO} = (PAR_{AED} - PAR_{BGD}) / PAR_{AED} \quad (5)$$

19 where AED is the above ecosystem downwelling PAR, AGD is the above grass downwelling PAR,
20 and BGD is the below grass downwelling PAR. We did not include the reflected component of PAR
21 in our calculations as this consistently produced negative fPAR results in the dry season. Once fPAR
22 was calculated, APAR was calculated for overstory, understory and ecosystem by multiplying the
23 respective fPAR with available incoming PAR (note: this was PAR_{AGD} for the understory).

24 The variability over time of vegetation LAI and biomass is a direct result of phenology and
25 productivity. We collected overstory LAI on each site visit (6 total) and understory biomass samples
26 spanning a full growing season (Dec-Apr, 4 total) to investigate how these variables changed
27 alongside the flux and phenocam data. We used digital hemispheric photography to record overstory
28 LAI using a Canon digital single lens reflex (DSLR) camera (Rebel T1i) with a 185 ° super fisheye
29 FOV (f/5.6) lens attached. A one hectare plot was established around the central ecosystem flux tower
30 and LAI measurements were recorded every 20 m within it (n = 36, Fig. 1). These images were
31 analysed using WinScanopy (v2014a), where a clumping coefficient was calculated to account for
32 foliage clumping in the LAI estimate.



1 A Tracing Radiation and Architecture of Canopies (TRAC) instrument was used to verify the
2 WinScanopy clumping index parameter, which agreed within 10-15 % of each other (0.82 to 0.94 in
3 the wet season, 0.61 to 0.67 in the dry season) and gave us confidence in the hemispheric LAI
4 estimates. Understory biomass below 2 m in height was collected from 20 replicate 1 x 1 m quadrats
5 along a N-S and E-W 100 m transect (10 samples each, every 5 m) and separated in the lab into grass
6 and other green biomass, weighed, then oven dried at 80 °C for 3 days to obtain a dry weight. The
7 exact distance of sampling along each transect was altered by 1 m for each site visit to avoid biasing
8 from the previous sampling period. Following the technique used by Chen et al. (2003), we converted
9 the dry weight biomass into carbon content assuming it to be 43 % of grass biomass and 49 % of other
10 green biomass.

11 2.5 Light use efficiency (LUE) models and incorporation of phenology

12 An alternative to estimating GPP from flux towers is to use a LUE model, where GPP is
13 approximated by relating plant productivity to the amount of light they absorb over a growing season
14 (Monteith, 1972). The MODIS GPP product (MOD17 A2/A3) is calculated using a LUE model (Eq.
15 (6), Running and Zhao, 2015), which we use in this study, as it has been previously validated for
16 Australian savannas (Kanniah et al., 2009):

$$17 \quad GPP = APAR \times LUE_p \times T_{MINscalar} \times VPDscalar \quad (6)$$

18 where GPP is in g C m⁻² d⁻¹, APAR is in MJ and LUE_p is peak light use efficiency in g C MJ⁻¹ PAR⁻¹.
19 Because C₃ (trees) and C₄ (grasses) plants have different maximum LUE rates (Zhu et al., 2008), we
20 calculated overstory and understory LUE_p separately following a similar approach to Kanniah et al.
21 (2009) and Coops et al. (2007), where LUE is firstly calculated as GPP/APAR and is then binned by
22 month to obtain monthly LUE. We chose to use the months of Dec-Mar (inclusive) to provide an
23 estimate of LUE_p for the overstory and understory, as these months ($n = 8$) have the least
24 environmental constraints to productivity and should be close to the maximum. This gave us a LUE_p
25 value of 1.49 ± 0.06 g C MJ⁻¹ PAR⁻¹ for the ecosystem, 1.22 ± 0.03 g C MJ⁻¹ PAR⁻¹ for the overstory
26 and 2.41 ± 0.23 g C MJ⁻¹ PAR⁻¹ for the understory (Fig. 3). In the LUE model the LUE_p values are
27 then down regulated on a daily basis using the VPD_{scalar} Eq. (7) and T_{MINscalar} (values between 0
28 and 1) Eq. (8) (Running and Zhao, 2015):

$$29 \quad VPDscalar = (VPD_{max} - VPD_d) / (VPD_{max} - VPD_{min}) \quad (7)$$

$$30 \quad T_{MINscalar} = (T_{MIN} - T_{MINmin}) / (T_{MINmax} - T_{MINmin}) \quad (8)$$

31 where T_{MIN} is the minimum daily temperature for a given day, T_{MINmax} is the minimum daily
32 temperature when LUE is at maximum and T_{MINmin} is the minimum daily temperature when LUE is 0,
33 all of which are output in °C. Likewise, VPD_d is the mean daytime VPD, VPD_{max} is the maximum



1 VPD when LUE is 0, and VPD_{min} is the minimum VPD when LUE is at maximum, all output in Pa.
2 These scalar values fall between the range of 0 – 1. The MOD17 GPP algorithm uses values of $-8^{\circ}C$
3 for T_{MINmin} , $11.39^{\circ}C$ for T_{MINmax} , 650 Pa for VPD_{min} and 3500 Pa for VPD_{max} for savannas (Running
4 and Zhao, 2015), so we also used these values for Howard Springs.

5 The use of a soil moisture term, evaporative fraction (EF), has been argued to represent plant
6 available moisture more reliably than VPD (Gentine et al., 2007; Yuan et al., 2007; Kanniah et al.,
7 2009). This term is simply a fractional estimate of latent heat (LE) divided by the sum of sensible heat
8 (H) and LE (i.e. $LE / (LE + H)$). We also used the EF term in this study to test if and how it improved
9 the estimation of overstory, understory and ecosystem GPP. For the overstory and ecosystem, we
10 calculated EF using the ecosystem flux tower, whereas for the understory we calculated EF using the
11 understory flux tower.

12 Another technique we tested for improving GPP estimates from the LUE model was to input
13 phenocam greenness indices, as they have been found to correlate with ecosystem productivity in
14 northern hemisphere forests and grasslands (Richardson et al., 2009b; Migliavacca et al.,
15 2011; Toomey et al., 2015). We hypothesised that inclusion of GCC in the LUE model would improve
16 the model's ability to predict savanna overstory and understory GPP, particularly given the strong
17 phenology cycles displayed in savannas. As GCC is a fractional measure, like that of fPAR, we
18 substituted GCC as a proxy for fPAR using the coefficients of a regression to normalise it, a similar
19 approach to that used by Migliavacca et al. (2011). As a result, Eq. 6 was transformed to include
20 $PAR \cdot (mGCC + c)$ in place of APAR, where m and c are the linear regression coefficients.

21 We repeated the above technique using MODIS EVI (Huete et al., 2002), to test if satellite indices
22 could be used to improve estimates of ecosystem scale GPP. We chose the EVI product
23 (MOD13Q1.005) as it has been shown to function well for identifying broad-scale phenology in
24 Australian savannas (Ma et al., 2013; Ma et al., 2014). A 3 x 3 pixel cut out of EVI data surrounding
25 the Howard Springs site, at 16-day and 250 m resolution, was processed in DINGO accepting the
26 quality flags 00 (highest overall quality) and 01 (good quality) only. The 16-day data were then
27 interpolated and smoothed, using a Savitzky-Golay technique (Savitzky and Golay, 1964) in DINGO,
28 to create a daily time series of EVI (Beringer et al., 2016b). Daily EVI were regressed against site-
29 based daily ecosystem fPAR and the regression was used to replace APAR in Eq. (6) to estimate
30 ecosystem GPP.

31 Finally, to test the performance of each model against tower GPP estimates, we used a Pearson
32 correlation to provide a closeness of fit estimate (Corr) and test if the relationship was statistically
33 significant ($p < 0.05$). We also calculated the root mean squared error (RMSE) to provide a measure of
34 the difference between the two datasets (tower and model) and the relative predictive error (RPE) to



- 1 represent the percentage difference between them, plus the degree of over- (+) or underestimation (-)
- 2 of the model.

3 3 Results & Discussion

4 3.1 Phenological insights from phenocams

5 Extraction of the chromatic coordinates and excess indexes revealed expected patterns from overstory
 6 and understory vegetation over time, showing that the cameras functioned well as phenology monitors
 7 of vegetation greenness at the ecosystem and individual species level (Fig. 4, 5 & 6). Not surprisingly,
 8 both GCC and ExG were at their highest in the understory during the wet season and gradually
 9 declined to their lowest values by the late dry season (i.e. September, Fig. 4). The RCC/ExR indices
 10 showed an inverse relationship to GCC/ExG, which is usually symptomatic of increased red
 11 pigmentation due to senescing leaves and chlorophyll loss (Hoch et al., 2001; Lee et al., 2003; Keenan
 12 et al., 2014). This relationship is shown by the red-green index crossover in the understory that
 13 coincides with grass senescence and signals the end of the wet season (i.e. Mar/Apr, see Fig. 4).
 14 However, in this case, the crossover is likely the combined result of grass senescence (loss of green)
 15 and an increase in the red kandosol soil background showing through with the loss of understory
 16 biomass.

17 A different story is depicted at the beginning of the wet season (Oct/Nov), whereby the red-green
 18 crossover does not occur as quickly as it does at the end of the wet season (Fig. 4). Here it occurs after
 19 several rainfall episodes in November (Fig. 4, Fig. 5 for rainfall). This is due to the time needed for
 20 the vegetation, particularly the grasses, to respond to the onset of the rainy season, as October and
 21 November are typically build up months where convective storms deliver rain in single events before
 22 the onset of the more consistent monsoonal rain in December (Cook and Heerdegen, 2001). Peak
 23 GCC and ExG are not reached until February (Fig. 4), which is also reflected in results from the
 24 biomass harvest (Table 1) that shows the mid wet season (February) to be the period of highest
 25 productivity for total understory biomass.

26 The understory consists of a mix of annual (*S. intrans*) and perennial (*S. plumosum* & *H. triticeous*)
 27 grasses, saplings of overstory (*E. tetradonta* & *E. miniata*) and mid-story (*E. chlorosyachys*, *T.*
 28 *ferdinandiana* & *B. obovata*) species and cycads (*C. armstrongii*) that all have differing phenologies
 29 (Bowman and Prior, 2005). The behaviour of these phenological guilds is reflected in the temporal
 30 patterns of GCC and ExG between grasses and the non-grass woody elements (herein referred to as
 31 'woody green') and provides additional insight into the dynamic nature of understory savanna
 32 phenology (Fig. 5). While grasses are considered the most abundant of the understory species in terms
 33 of biomass (Table 1) and LAI at Howard Springs (Hutley et al., 2000), they are only active during the
 34 wet season months (Andrew and Mott, 1983; Scott et al., 2010). During both the early dry season



1 (April/May) and after the first rains of the wet season (October/November), the woody green species
2 take advantage of the lack of grass to gain biomass (Werner and Franklin, 2010; Werner and Prior,
3 2013).

4 Annual grasses typically germinate after the first 15 mm or more of rainfall, with further rainfall
5 events required to drive leaf growth (Andrew and Mott, 1983; Cook et al., 2002). Pre-monsoonal
6 rainfall is highly variable in terms of its timing and amount, therefore this phenological strategy may
7 minimise the possibility of grass mortality if dry periods proceed an initial early wet season rainfall
8 event (Mott, 1978). In Fig. 5, this delay in grass greening is evident, with rapid increases in GCC only
9 occurring approximately a month after the first rainfall event (Fig. 5, Oct-Dec 2013). Such detailed
10 analysis of the phenocam data can tease apart composite greening signals to better understand
11 phenological dynamics and fluxes (Fig. 5 & 7). Results from understory biomass harvests also support
12 the GCC results, revealing that as the wet season progressed, grass biomass increased in dominance to
13 account for 77 % of understory biomass by the end of the wet season (Table 1). This shows that while
14 the grasses are the primary driver of understory biomass and productivity, the woody green species
15 also make important contributions throughout the year and are likely the reason why understory GPP
16 does not completely cease in the dry season (Moore et al., 2016a).

17 In contrast to the understory, the overstory GCC and ExG did not fluctuate much in comparison to
18 their red and blue channel indices (Fig. 6, a). This is mostly due to the high portion of blue sky and
19 cloud within the ROI's for the overstory images (Fig. 2, e & f), which vary depending on daily
20 weather conditions. The effect on BCC/ExB is particularly strong during the wet season, where the
21 summer monsoon varies sky conditions considerably between bright blue sky and dull grey cloud.
22 Due to the narrow FOV and upward orientation of the overstory cameras, the trees were prone to
23 moving in and out of smaller ROI tested (data not shown), so a larger ROI was chosen to ensure tree
24 foliage was always present in the image, but at the cost of including a greater sky portion (Fig. 2, e &
25 f).

26 Nevertheless, when viewed in isolation from the red and blue indices, temporal variation was apparent
27 in overstory GCC and ExG. These indices captured the variability in greenness and were consistent
28 with changes in overstory LAI when compared with adhoc hemispherical LAI measurements (Fig. 6,
29 b). While there is inherent uncertainty in both the phenocam imagery (i.e. FOV, scene illumination)
30 and LAI (i.e. leaf projection and orientation, clumping, gaps, see Ryu et al. (2010)) estimates in this
31 study, the savanna tree canopy is known to experience seasonal fluctuations in LAI with the highest
32 values in the wet season and lowest values in the late dry season (Williams et al., 1997; O'Grady et al.,
33 2000). The same general pattern is displayed in Fig. 6, giving us confidence that the phenocams are
34 able to detect overstory cover change, despite their limitations in setup and image collection.



1 3.2 Integrating phenocam and MODIS phenology with GPP

2 The seasonality of GPP in these savannas has been found to differ between that of the overstory and
3 understory, with understory GPP tied more closely to the duration of the wet season than that of the
4 overstory (Moore et al., 2016a). The GCC and ExG time series approximated the overstory and
5 understory GPP estimates well (Fig. 7), and we hypothesise that they could be useful for
6 independently predicting overstory and understory GPP. Simple linear regressions of GCC against
7 flux tower GPP quantified the relationship between the two variables, with understory GPP ($r^2 = 0.65$)
8 revealing a closer fit with GCC than overstory GPP ($r^2 = 0.23$, Fig. 7). The ExG index did not perform
9 so well compared with GCC for the overstory ($r^2 = 0.09$) but improved the relationship slightly
10 against GCC for the understory ($r^2 = 0.70$, Fig. 7). ExG was originally developed for identifying green
11 vegetation from images with a soil background (Woebbecke et al., 1995). This is a likely reason for
12 why the relationship between ExG and GPP was slightly closer to 1:1 than that of GCC for the
13 understory.

14 While the relationship between overstory greenness (ExG/GCC) and GPP is not as strong as that of
15 the understory, the phenocams are still able to detect seasonality in greenness that follows GPP over
16 time (Fig. 7). The trees have a deeper rooting structure than the grasses, allowing them to access a
17 larger volume of soil moisture (Eamus et al., 2002; Kelley et al., 2007) and thus maintain constant
18 overstory transpiration throughout the year (O'Grady et al., 1999; Hutley et al., 2000). While the tree
19 canopy is largely evergreen, the LAI will drop up to 30-40 % in order to account for the dry season
20 water deficit (O'Grady et al., 2000; Whitley et al., 2011), which is also apparent from both our
21 overstory LAI and GCC results (Fig. 6). Tree productivity, in contrast to transpiration, is known to
22 decrease into the dry season (Eamus et al., 1999), and most carbon uptake is directed toward
23 maintenance respiration rather than growth (Chen et al., 2002; Prior et al., 2004; Cernusak et al., 2006).
24 However, the occurrence of late wet season rainfall events may benefit the productive capacity of the
25 trees by boosting soil moisture stores, thereby supporting higher rates of productivity for longer in the
26 dry season (Moore et al., 2016a). This effect is apparent in our overstory GCC time series, where after
27 late April to early May rainfall events (see Fig. 5 for daily rainfall), GCC spikes in June indicate a
28 flushing of the foliage in the dry season (Fig. 6, b).

29 At the ecosystem scale, the interaction of the overstory and understory with the wet and dry seasons
30 drives variability in productivity. The MODIS greenness index, EVI, mostly captures this variability,
31 albeit at coarser temporal resolution (Fig. 7, e) when compared with the phenocams. While the broad
32 scale variability in savanna phenology change is captured by EVI, such as seasonality (Ma et al.,
33 2013), it is not able to capture the finer scale details that the site based phenocams can. MODIS
34 indices, such as EVI, do not currently have the ability to identify individual plant scale phenology
35 patterns (Brown et al., 2016; Moore et al., 2016b), which is another advantage of the phenocam (Fig.
36 5). The phenocam data also provides a useful means of validating the MODIS data in that both are



1 able to track the seasonality of savanna GPP, which is driven by a complex interaction of both
2 meteorology and phenology (Kanniah et al., 2011;Whitley et al., 2011;Ma et al., 2013;Ma et al.,
3 2014).

4 **3.3 Integrating phenocam and MODIS phenology with a LUE model**

5 In order to test the applicability of the phenocam indices and MODIS EVI to independently predict
6 savanna GPP using a LUE model, peak LUE (i.e. LUE_p) needed to be calculated for the ecosystem,
7 overstory and understory. The calculated LUE_p value was higher for the understory ($2.41 \pm 0.23 \text{ g C}$
8 $\text{MJ}^{-1} \text{ PAR}^{-1}$) compared to the overstory ($1.22 \pm 0.03 \text{ g C MJ}^{-1} \text{ PAR}^{-1}$, Fig. 3). The higher LUE_p for the
9 understory is largely due to the dominance of C_4 grasses in the understory (Table 1), as their C_4
10 photosynthetic pathway is more energy efficient (Sage, 2004;Osborne and Beerling, 2006;Zhu et al.,
11 2008). Our values fell within the range of LUE_p reported for African savannas, which have varied
12 from as low as $0.33 \text{ g C MJ}^{-1} \text{ PAR}^{-1}$ up to $3.5 \text{ g C MJ}^{-1} \text{ PAR}^{-1}$ depending on the vegetation and season
13 (Sjöström et al., 2013;Tagesson et al., 2015). Recent work has shown the importance of correctly
14 applying LUE_p values to C_3 and C_4 plants when using LUE models to calculate GPP (Yan et al., 2015).
15 Therefore, to account for the C_3 : C_4 differences, we applied these site and trait specific values to the
16 LUE model used to estimate GPP.

17 The next step in our parameterisation of the LUE model was to test it in its traditional form; using the
18 meteorological inputs of T_{MIN} and VPD that constrain LUE_p , along with APAR (Eq. 6). We found the
19 model captured most of the seasonality of overstory GPP but underestimated the magnitude of GPP in
20 the dry season and overestimated GPP in the wet season (Table 2, Fig. 8, a). For the understory, the
21 LUE model appeared to overestimate and lag flux tower GPP consistently by 1-2 months (Table 2,
22 Fig. 9, a). This resulted in a strong dry season over estimate of understory GPP (159 %, Table 2). For
23 the ecosystem, the LUE model consistently overestimated GPP (Table 2, Fig. 10, a). Kanniah et al.
24 (2009) also found the LUE model performed poorly for the Howard Springs ecosystem, so they
25 replaced the standard VPD parameterisation with an EF term and found this to improve the
26 relationship, which we implemented next.

27 Application of EF to the overstory model in this study improved its ability to predict GPP in the dry
28 season but overestimated GPP in the wet season, causing an over prediction of annual GPP by 8 %
29 overall (Table 2, Fig. 8, a vs. b). In contrast, the inclusion of EF in the understory LUE model slightly
30 improved the prediction of annual GPP, with better correlation (0.73 vs 0.57), lower RMSE (1.43 vs.
31 2.02 g C m^{-2}) and lower RPE (22.27 vs. 62.09 %). However, the understory model still lagged tower
32 GPP and was still particularly poor at capturing the seasonal transitions (Fig. 9 a & b). For the
33 ecosystem, the inclusion of EF enhanced the overestimation of GPP from 14 to 25 %, particularly in
34 the wet season (Table 2, Fig. 10, a vs. b). EF provides a proxy measure of soil moisture as it includes
35 a water flux component (LE) that is tightly linked with soil moisture availability (Gentine et al.,



1 2007;Kanniah et al., 2009). In Australian savannas, soil moisture is highly seasonal and a major driver
2 of productivity (Kanniah et al., 2010). This makes EF a useful index in the dry season, when latent
3 heat largely comes from transpiration and is therefore tightly coupled with GPP. However, in the wet
4 season, soil evaporation contributes a large amount to latent heat, which is not tightly coupled to GPP
5 (Kanniah et al., 2009). This explains why EF is able to constrain the LUE model in the dry season and
6 why it performs poorly in the wet season and transition periods.

7 The incorporation of phenocam GCC into the LUE model improved the estimate of understory GPP
8 substantially (Table 2, Fig. 9, c & d). This was most apparent with the combined use of GCC and EF
9 in the LUE model, which produced the best correlation ($r = 0.85$), lowest RMSE (0.96 g C m^{-2}) and
10 lowest RPE (17.73 %, Table 2, Fig. 9). These results show that while EF is an important factor for
11 GPP, greenness phenology is also key for estimating understory productivity. In further support of
12 this, the inclusion of GCC also eliminated the lag in model estimated GPP, bringing the estimate
13 closer in line with seasonal variability from the flux tower, as evidenced by the large decrease in
14 RMSE and RPE (Table 2, Fig. 9). As previously discussed, the understory grasses (annual species in
15 particular) die off at the cessation of the wet season and do not contribute to the small fraction of
16 understory GPP in the dry season (Moore et al., 2016a). This is a plant phenology response, rather
17 than a response to meteorological conditions, as factors such as soil moisture remain high enough in
18 the early dry season to support plant growth (Eamus et al., 2002;Kelley et al., 2007;Moore et al.,
19 2016a). Given that these grasses dominate understory biomass at Howard Springs, it is not surprising
20 that including greenness phenology information in the LUE model improves its output relative to the
21 flux tower.

22 The inclusion of greenness indices in the LUE model for the overstory (GCC) and ecosystem (EVI)
23 also improved the estimate of GPP. For the overstory, the combination of EF and GCC performed
24 slightly better in the dry season than GCC alone, but was not able to capture the wet season well
25 (Table 2, Fig. 8 d). This resulted in the incorporation of GCC into the LUE model producing the best
26 overall result, despite the slightly lower correlation value (0.60 vs 0.72) and RMSE (1.43 vs. 1.36 g C
27 m^{-2}) when compared with GCC and EF combined (Table 2). For the ecosystem, the inclusion of EVI
28 into the LUE model performed the best at predicting GPP, which was supported by the lowest values
29 for RMSE (2.03 g C m^{-2}) and RPE (13.76 %, Table2).

30 The greenness information clearly fills an important gap in relation to changes in overstory,
31 understory and ecosystem greenness. The general improvement in LUE model output for overstory,
32 understory and ecosystem with the inclusion of greenness phenology information highlights the
33 importance of accounting for phenological variability when estimating GPP in savannas. A similar
34 result was found for a subalpine grassland in Italy, where phenocam greenness indices improved the
35 ability of the same LUE model to predict grassland GPP (Migliavacca et al., 2011). Likewise, in an



1 evergreen Amazonian rainforest, Wu et al. (2016) linked phenological changes in leaf development
2 and demography to seasonality in GPP, showing the importance of phenology as a driver of
3 ecosystem productivity. For Australian savannas, the effect of phenology is most evident at the end of
4 the wet season (Apr-May), where in the understory, growth ceases due to annual grass senescence
5 even though meteorological conditions (temperature, VPD and/or EF) are still sufficient to support
6 growth (Fig. 9 a&b vs. c&d). The original LUE model over-predicts GPP as a result of this, which is
7 substantially reduced by the inclusion of greenness phenology indices.

8 **3.4 Limitations, impacts and further work**

9 While phenocams have consistently proven to be a useful tool for phenological and productivity
10 research (Richardson et al., 2009b; Migliavacca et al., 2011; Toomey et al., 2015; Wu et al., 2016),
11 there still remain several limitations that require further investigation to improve their utility. Issues
12 related to camera choice and image collection have been shown to be less problematic for simple
13 identification of phenological transition dates and seasonal variation than first thought (Sonnentag et
14 al., 2012), however, maintaining similar protocols for cross site comparisons remains preferable
15 (Moore et al., 2016b). Scene illumination variability is probably the most problematic limitation of
16 phenocams, which can be reduced by using chromatic coordinates or excess values, as well as by
17 setting the white balance to a fixed level (Richardson et al., 2009a; Ide and Oguma, 2010; Migliavacca
18 et al., 2011). Although white balance was not fixed for this study, we found that the GCC and ExG
19 time series matched well with GPP estimates regardless and provided added value to that gained from
20 using just APAR alone in the LUE model.

21 The wet season influence on scene illumination adds daily noise to the time series, but the indices are
22 still useful for informing seasonal productivity estimates. This same relationship will likely not stand
23 for other, less dynamic ecosystems in Australia (Restrepo-Coupe et al., 2015; Moore et al., 2016b), so
24 we recommend the fixing of white balance where appropriate. The use of a grey reference panel for
25 normalising phenocam images has also been proposed (Richardson et al., 2009a), however, this
26 technique has issues related to panel orientation and illumination conditions that can be different to
27 those experienced by the phenocams (Migliavacca et al., 2011). Despite these limitations, phenocams
28 are still an important tool for both species and plot scale phenology monitoring and with further
29 developments, will continue to provide valuable insight into Australian vegetation phenology (Moore
30 et al., 2016b).

31 In addition to the phenocam issues, the light use efficiency model used in this study is also subject to
32 limitations. This model relies on the input of meteorological information to generate an estimate of
33 ecosystem GPP. It is often found that these models overestimate GPP in the transition periods from
34 wet-dry or dry-wet in savanna ecosystems (Kanniah et al., 2009). The primary reason for this is that
35 savanna GPP is not driven solely by meteorology, that plant phenology also plays an important role,



1 as shown in our analysis. The technique for estimating LUE_p , used in the LUE model (Eq. 5), also
 2 involves a degree of uncertainty that is centred around the input parameters of LUE and APAR, as
 3 well as the scalars used to constrain it (Heinsch et al., 2006; Sjöström et al., 2013).

4 The MODIS MOD17 A2/A3 GPP product uses a LUE_p value of 1.21 g C MJ^{-1} for savannas and 1.24
 5 g C MJ^{-1} for woody savannas (Zhao and Running, 2010). While these values are close to the number
 6 we calculated for the overstory ($1.26 \pm 0.03 \text{ g C MJ}^{-1} \text{ PAR}^{-1}$), we found the understory LUE_p to be
 7 much larger ($2.44 \pm 0.23 \text{ g C MJ}^{-1} \text{ PAR}^{-1}$). Similarly, for African savannas, LUE_p has been found to
 8 reach up to $3.50 \text{ g C MJ}^{-1} \text{ PAR}^{-1}$ in the wet (growing) season (Sjöström et al., 2013; Tagesson et al.,
 9 2015). These LUE_p values are much larger than that used in the MOD17 A2/A3 algorithm, which
 10 suggests that tree-grass (C_3 vs. C_4) ratios need to be better accounted for in the LUE model. Recent
 11 work from Yan et al. (2015) has shown this to be the case, where the application of different LUE_p
 12 values to C_3 ($1.8 \text{ g C MJ}^{-1} \text{ PAR}^{-1}$) and C_4 ($2.76 \text{ g C MJ}^{-1} \text{ PAR}^{-1}$) plants improved global model
 13 estimates of GPP.

14 Finally, the flux tower estimates of GPP are not without their own limitations, as the towers measure
 15 NEE that is then partitioned into GPP and respiration most commonly by using a friction velocity (u^*)
 16 threshold at night and upscaling method for the daytime (Reichstein et al., 2005; Lasslop et al.,
 17 2012; Barr et al., 2013). Use of the u^* technique has been shown to be problematic at sites with
 18 complex terrain (van Gorsel et al., 2009), where drainage flows result in horizontal loss of carbon
 19 from an ecosystem that is not accounted for by the flux instruments. While Howard Springs is a
 20 relatively flat site (slope $< 1^\circ$) that should prevent issues with using the u^* technique, the flux tower
 21 estimates from this site should still be considered with an amount of uncertainty as well (Moore et al.,
 22 2016a; McHugh et al., In Submission). However, these issues have been addressed by previous work
 23 at this site (Moore et al., 2016a) so we have confidence in the fluxes used for this study. Despite these
 24 limitations, we were able to show that the input of phenological information into LUE models can
 25 provide a useful constraint for estimating GPP within the uncertainty limits of tower derived estimates,
 26 a similar conclusion to that found over a subalpine grassland in the Italian Alps (Migliavacca et al.,
 27 2011).

28 **4 Conclusion**

29 We have shown the utility of phenocams for the monitoring of tree and grass phenology in savannas
 30 and how this data can improve the quantification of productivity. Phenocams offer the ability to
 31 decipher species level phenological signals, as shown by our time series analysis of understory grasses
 32 and woody green species, as well as in the tracking of seasonal overstory leaf area change. Phenocams
 33 have also shown to be useful for improving LUE models that have traditionally failed to capture the
 34 wet-dry season transition periods well in savannas, which are characterised by phenology changes in



1 the understory that are out of sync with meteorological variability. This approach needs to be tested in
2 more ecosystems to determine its applicability for a wider range of ecosystem types, but promises
3 improved results for better understanding of ecosystem GPP and phenology. Phenological information
4 offers an important link for our understanding of ecosystem function as it provides a more accurate
5 means of independently verifying tower derived GPP estimates in savannas. We have demonstrated
6 that phenocams can be used in conjunction with eddy covariance flux towers to improve current
7 knowledge of savanna productivity and phenology, which will assist in our understanding of how the
8 tree-grass relationship in savannas may alter in the future.

9 **Author Contributions**

10 Field work and experimental design was executed by C. Moore, J. Beringer, L. Hutley and B. Evans.
11 Data analysis was chiefly carried out by C. Moore, with some coding assistance from B. Evans. The
12 manuscript was prepared by C. Moore with contributions from all co-authors.

13 **Acknowledgements**

14 Firstly, the authors would like to acknowledge support and funding from OzFlux and the overarching
15 Terrestrial Ecosystem Research Network (TERN), which is supported by the Australian Government
16 through the National Collaborative Research Infrastructure Strategy. This work utilised data collected
17 by grants funded by the Australian Research Council (DP0344744, DP0772981 and DP130101566).
18 Beringer is funded under an ARC FT (FT110100602). B. Evans is funded by the TERN Ecosystem
19 Modelling and Scaling Infrastructure. Special thanks are also made to Dr Peter Isaac for his
20 development of the OzFluxQC standardised processing tools and to Mr. Matthew Northwood for his
21 design and building of the mini towers and for his assistance with field work.

22

23

24



References

- Andrew, M. H., and Mott, J. J.: Annuals with transient seed banks: the population biology of indigenous *Sorghum* species of tropical north-west Australia, *Australian Journal of Ecology*, 8, 265-276, 1983.
- Baldocchi, D., Falge, E., Gu, L., Olson, R., Hollinger, D., Running, S., Anthoni, P., Bernhofer, C., Davis, K., Evans, R., Fuentes, J., Goldstein, A., Katul, G., Law, B., Lee, X., Malhi, Y., Meyers, T., Munger, W., Oechel, W., Paw, U. K. T., Pilegaard, K., Schmid, H. P., Valentini, R., Verma, S., Vesala, T., Wilson, K., and Wofsy, S.: FLUXNET: A New Tool to Study the Temporal and Spatial Variability of Ecosystem-Scale Carbon Dioxide, Water Vapor, and Energy Flux Densities, *Bulletin of the American Meteorological Society*, 82, 2415-2434, 2001.
- Baret, F., de Solan, B., Lopez-Lozano, R., Ma, K., and Weiss, M.: GAI estimates of row crops from downward looking digital photos taken perpendicular to rows at 57.5° zenith angle: Theoretical considerations based on 3D architecture models and application to wheat crops, *Agricultural and Forest Meteorology*, 150, 1393-1401, 10.1016/j.agrformet.2010.04.011, 2010.
- Barr, A. G., Richardson, A. D., Hollinger, D. Y., Papale, D., Arain, M. A., Black, T. A., Bohrer, G., Dragoni, D., Fischer, M. L., Gu, L., Law, B. E., Margolis, H. A., McCaughey, J. H., Munger, J. W., Oechel, W., and Schaeffer, K.: Use of change-point detection for friction-velocity threshold evaluation in eddy-covariance studies, *Agricultural and Forest Meteorology*, 171-172, 31-45, 10.1016/j.agrformet.2012.11.023, 2013.
- Beringer, J., Hutley, L. B., Tapper, N. J., and Cernusak, L. A.: Savanna fires and their impact on net ecosystem productivity in North Australia, *Global Change Biology*, 13, 990-1004, 2007.
- Beringer, J., Hutley, L. B., Abramson, D., Arndt, S. K., Briggs, P., Bristow, M., Canadell, J. G., Cernusak, L. A., Eamus, D., Edwards, A. C., Evans, B. J., Fest, B., Goergen, K., Grover, S. P., Hacker, J., Haverd, V., Kanniah, K., Livesley, S. J., Lynch, A., Maier, S., Moore, C., Raupach, M., Russell-Smith, J., Scheiter, S., Tapper, N. J., and Uotila, P.: Fire in Australian savannas: From leaf to landscape, *Global Change Biology*, 21, 62-81, 2015.
- Beringer, J., Hutley, L., McHugh, I., Arndt, S., Campbell, D., Cleugh, H., Cleverly, J., Resco de Dios, V., Eamus, D., Evans, B., Ewenz, C., Grace, P., Griebel, A., Haverd, V., Hinko-Najera, N., Isaac, P., Kanniah, K., Leuning, R., Liddell, M., Macfarlane, C., Meyer, W., Moore, C., Pendall, E., Phillips, A., Phillips, R., Prober, S., Restrepo-Coupe, N., Rutledge, S., Schroder, I., Silberstein, R., Southall, P., Sun, M., Tapper, N., van Gorsel, E., Vote, C., Walker, J., and Wardlaw, T.: An introduction to the Australian and New Zealand flux tower network - OzFlux, *Biogeosciences Discuss.*, 2016a.
- Beringer, J., McHugh, I., and Kljun, N.: Dynamic INtegrated Gap filling and partitioning for OzFlux (DINGO), *Biogeosciences Discuss.*, doi:10.5194/bg-2016-188, 2016b.
- Bond, W. J., Midgley, G. F., and Woodward, F. I.: The importance of low atmospheric CO₂ and fire in promoting the spread of grasslands and savannas, *Global Change Biology*, 9, 973-982, 2003.
- Bond, W. J.: What limits trees in C₄ grasslands and savannas?, *Annual Review of Ecology, Evolution, and Systematics*, 39, 641-659, 2008.
- Bowman, D. M. J. S., and Prior, L. D.: Why do evergreen trees dominate the Australian seasonal tropics?, *Australian Journal of Botany*, 53, 379-399, 2005.



Broich, M., Huete, A., Paget, M., Ma, X., Tulbure, M., Coupe, N. R., Evans, B., Beringer, J., Devadas, R., Davies, K., and Held, A.: A spatially explicit land surface phenology data product for science, monitoring and natural resources management applications, *Environmental Modelling & Software*, 64, 191-204, <http://dx.doi.org/10.1016/j.envsoft.2014.11.017>, 2015.

Brown, T. B., Hultine, K. R., Steltzer, H., Denny, E. G., Denslow, M. W., Granados, J., Henderson, S., Moore, D., Nagai, S., Sanclements, M., Sánchez-Azofeifa, A., Sonnentag, O., Tazik, D., and Richardson, A. D.: Using phenocams to monitor our changing earth: Toward a global phenocam network, *Frontiers in Ecology and the Environment*, 14, 84-93, 10.1002/fee.1222, 2016.

Cernusak, L. A., Hutley, L. B., Beringer, J., and Tapper, N. J.: Stem and leaf gas exchange and their responses to fire in a north Australian tropical savanna, *Plant, Cell and Environment*, 29, 632-646, 2006.

Chen, X., Eamus, D., and Hutley, L. B.: Seasonal patterns of soil carbon dioxide efflux from a wet-dry tropical savanna of northern Australia, *Australian Journal of Botany*, 50, 43-51, 2002.

Chen, X., Hutley, L. B., and Eamus, D.: Carbon balance of a tropical savanna of northern Australia, *Oecologia*, 137, 405-416, 2003.

Cook, G. D., and Heerdegen, R. G.: Spatial variation in the duration of the rainy season in monsoonal Australia, *International Journal of Climatology*, 21, 1723-1732, 2001.

Cook, G. D., Williams, R. J., Hutley, L. B., O'Grady, A. P., and Liedloff, A. C.: Variation in vegetative water use in the savannas of the North Australian Tropical Transect, *Journal of Vegetation Science*, 13, 413-418, 2002.

Coops, N. C., Black, T. A., Jassal, R. S., Trofymow, J. A., and Morgenstern, K.: Comparison of MODIS, eddy covariance determined and physiologically modelled gross primary production (GPP) in a Douglas-fir forest stand, *Remote Sensing of Environment*, 107, 385-401, 10.1016/j.rse.2006.09.010, 2007.

Eamus, D., Myers, B., Duff, G., and Williams, D.: Seasonal changes in photosynthesis of eight savanna tree species, *Tree Physiology*, 19, 665-671, 1999.

Eamus, D., Hutley, L. B., and O'Grady, A. P.: Daily and seasonal patterns of carbon and water fluxes above a north Australian savanna, *Tree Physiology*, 21, 977-988, 2001.

Eamus, D., Chen, X., Kelley, G., and Hutley, L. B.: Root biomass and root fractal analyses of an open Eucalyptus forest in a savanna of north Australia, *Australian Journal of Botany*, 50, 31-41, 2002.

Eberhardt, I. D. R., Schultz, B., Rizzi, R., Sanches, I. D., Formaggio, A. R., Atzberger, C., Mello, M. P., Immitzer, M., Trabaquini, K., Foschiera, W., and Luiz, A. J. B.: Cloud cover assessment for operational crop monitoring systems in tropical areas, *Remote Sensing*, 8, doi:10.3390/rs8030219, 2016.

Gentine, P., Entekhabi, D., Chehbouni, A., Boulet, G., and Duchemin, B.: Analysis of evaporative fraction diurnal behaviour, *Agricultural and Forest Meteorology*, 143, 13-29, 10.1016/j.agrformet.2006.11.002, 2007.

Gillespie, A. R., Kahle, A. B., and Walker, R. E.: Color enhancement of highly correlated images. II. Channel ratio and "chromaticity" transformation techniques, *Remote Sensing of Environment*, 22, 343-365, 1987.



Grace, J., José, J. S., Meir, P., Miranda, H. S., and Montes, R. A.: Productivity and carbon fluxes of tropical savannas, *Journal of Biogeography*, 33, 387-400, 2006.

Hanan, N. P., and Lehmann, C. E. R.: Tree-Grass interactions in savannas: Paradigms, contradictions and conceptual models, in: *Ecosystem Function in Savannas*, edited by: Hill, M. J., and Hanan, N. P., CRC Press, Florida, 2010.

Heinsch, F. A., Zhao, M., Running, S. W., Kimball, J. S., Nemani, R. R., Davis, K. J., Bolstad, P. V., Cook, B. D., Desai, A. R., Ricciuto, D. M., Law, B. E., Oechel, W. C., Kwon, H., Luo, H., Wofsy, S. C., Dunn, A. L., Munger, J. W., Baldocchi, D. D., Xu, L., Hollinger, D. Y., Richardson, A. D., Stoy, P. C., Siqueira, M. B. S., Monson, R. K., Burns, S. P., and Flanagan, L. B.: Evaluation of remote sensing based terrestrial productivity from MODIS using regional tower eddy flux network observations, *IEEE Transactions on Geoscience and Remote Sensing*, 44, 1908-1923, 10.1109/TGRS.2005.853936, 2006.

Hoch, W. A., Zeldin, E. L., and McCown, B. H.: Physiological significance of anthocyanins during autumnal leaf senescence, *Tree Physiology*, 21, 1-8, 2001.

Hoffmann, W. A., Geiger, E. L., Gotsch, S. G., Rossatto, D. R., Silva, L. C. R., Lau, O. L., Haridasan, M., and Franco, A. C.: Ecological thresholds at the savanna-forest boundary: How plant traits, resources and fire govern the distribution of tropical biomes, *Ecology Letters*, 15, 759-768, 2012.

Huete, A., Didan, K., Miura, T., Rodriguez, E. P., Gao, X., and Ferreira, L. G.: Overview of the radiometric and biophysical performance of the MODIS vegetation indices, *Remote Sensing of Environment*, 83, 195-213, 2002.

Hufkens, K., Friedl, M., Sonnentag, O., Braswell, B. H., Milliman, T., and Richardson, A. D.: Linking near-surface and satellite remote sensing measurements of deciduous broadleaf forest phenology, *Remote Sensing of Environment*, 117, 307-321, 10.1016/j.rse.2011.10.006, 2012.

Hutley, L., and Beringer, J.: Disturbance and climatic drivers of carbon dynamics of a north Australian tropical savanna, in: *Ecosystem Function in Savannas: Measurements and Modelling at Landscape to Global Scales*, edited by: Hill, M. J., and Hanan, N. P., CRC Press, Boca Raton, 57-75, 2011.

Hutley, L. B., O'Grady, A. P., and Eamus, D.: Evapotranspiration from eucalypt open-forest savanna of northern australia, *Functional Ecology*, 14, 183-194, 2000.

Hutley, L. B., Beringer, J., Isaac, P. R., Hacker, J. M., and Cernusak, L. A.: A sub-continental scale living laboratory: Spatial patterns of savanna vegetation over a rainfall gradient in northern Australia, *Agricultural and Forest Meteorology*, 151, 1417-1428, 2011.

Hutley, L. B., Evans, B. J., Beringer, J., Cook, G. D., Maier, S. W., and Razon, E.: Impacts of an extreme cyclone event on landscape-scale savanna fire, productivity and greenhouse gas emissions, *Environmental Research Letters*, 8, 1-12, 2013.

Ide, R., and Oguma, H.: Use of digital cameras for phenological observations, *Ecological Informatics*, 5, 339-347, 10.1016/j.ecoinf.2010.07.002, 2010.

Isbell, R. F.: *The Australian Soil Classification*, CSIRO Publishing, Collingwood, VIC, 1996.

Kaimal, J. C., and Finnigan, J. J.: *Atmospheric boundary layer flows: their structure and measurement*, Oxford University Press, New York, 1994.



Kanniah, K. D., Beringer, J., Hutley, L. B., Tapper, N. J., and Zhu, X.: Evaluation of Collections 4 and 5 of the MODIS Gross Primary Productivity product and algorithm improvement at a tropical savanna site in northern Australia, *Remote Sensing of Environment*, 113, 1808-1822, 2009.

Kanniah, K. D., Beringer, J., and Hutley, L. B.: The comparative role of key environmental factors in determining savanna productivity and carbon fluxes: A review, with special reference to Northern Australia, *Progress in Physical Geography*, 34, 459-490, 2010.

Kanniah, K. D., Beringer, J., and Hutley, L. B.: Environmental controls on the spatial variability of savanna productivity in the Northern Territory, Australia, *Agricultural and Forest Meteorology*, 151, 1429-1439, 2011.

Keenan, T. F., Darby, B., Felts, E., Sonnentag, O., Friedl, M. A., Hufkens, K., O'Keefe, J., Klosterman, S., Munger, J. W., Toomey, M., and Richardson, A. D.: Tracking forest phenology and seasonal physiology using digital repeat photography: A critical assessment, *Ecological Applications*, 24, 1478-1489, 2014.

Kelley, G., O'Grady, A. P., Hutley, L. B., and Eamus, D.: A comparison of tree water use in two contiguous vegetation communities of the seasonally dry tropics of northern Australia: The importance of site water budget to tree hydraulics, *Australian Journal of Botany*, 55, 700-708, 10.1071/BT07021, 2007.

Lasslop, G., Migliavacca, M., Bohrer, G., Reichstein, M., Bahn, M., Ibrom, A., Jacobs, C., Kolari, P., Papale, D., Vesala, T., Wohlfahrt, G., and Cescatti, A.: On the choice of the driving temperature for eddy-covariance carbon dioxide flux partitioning, *Biogeosciences*, 9, 5243-5259, 10.5194/bg-9-5243-2012, 2012.

Lee, D. W., O'Keefe, J., Holbrook, N. M., and Feild, T. S.: Pigment dynamics and autumn leaf senescence in a New England deciduous forest, eastern USA, *Ecological Research*, 18, 677-694, 2003.

Lehmann, C. E. R., Anderson, T. M., Sankaran, M., Higgins, S. I., Archibald, S., Hoffmann, W. A., Hanan, N. P., Williams, R. J., Fensham, R. J., Felfili, J., Hutley, L. B., Ratnam, J., San Jose, J., Montes, R., Franklin, D., Russell-Smith, J., Ryan, C. M., Durigan, G., Hiernaux, P., Haidar, R., Bowman, D. M. J. S., and Bond, W. J.: Savanna vegetation-fire-climate relationships differ among continents, *Science*, 343, 548-552, 2014.

Leuning, R., van Gorsel, E., Massman, W. J., and Isaac, P. R.: Reflections on the surface energy imbalance problem, *Agricultural and Forest Meteorology*, 156, 65-74, 2012.

Ma, X., Huete, A., Yu, Q., Coupe, N. R., Davies, K., Broich, M., Ratana, P., Beringer, J., Hutley, L. B., Cleverly, J., Boulain, N., and Eamus, D.: Spatial patterns and temporal dynamics in savanna vegetation phenology across the north Australian tropical transect, *Remote Sensing of Environment*, 139, 97-115, 2013.

Ma, X., Huete, A., Yu, Q., Restrepo-Coupe, N., Beringer, J., Hutley, L. B., Kanniah, K. D., Cleverly, J., and Eamus, D.: Parameterization of an ecosystem light-use-efficiency model for predicting savanna GPP using MODIS EVI, *Remote Sensing of Environment*, 154, 253-271, 10.1016/j.rse.2014.08.025, 2014.

McHugh, I., Beringer, J., Cunningham, S., Baker, P. J., Cavagnaro, T. R., MacNally, R. C., and Thompson, R. M.: Interactions between nocturnal turbulent flux, storage and advection at an 'ideal' Eucalypt woodland site., *Biogeosciences Discuss.*, In Submission.

Migliavacca, M., Galvagno, M., Cremonese, E., Rossini, M., Meroni, M., Sonnentag, O., Cogliati, S., Manca, G., Diotri, F., Busetto, L., Cescatti, A., Colombo, R., Fava, F., Morra di Cella, U., Pari, E.,



- Siniscalco, C., and Richardson, A. D.: Using digital repeat photography and eddy covariance data to model grassland phenology and photosynthetic CO₂ uptake, *Agricultural and Forest Meteorology*, 151, 1325-1337, 2011.
- Monteith, J. L.: Solar Radiation and Productivity in Tropical Ecosystems, *Journal of Applied Ecology*, 9, 747-766, 10.2307/2401901, 1972.
- Moore, C. E., Beringer, J., Evans, B., Hutley, L. B., McHugh, I., and Tapper, N. J.: The contribution of trees and grasses to productivity of an Australian tropical savanna, *Biogeosciences*, 13, 2387-2403, doi:10.5194/bg-13-2387-2016, 2016a.
- Moore, C. E., Brown, T., Keenan, T., Duursma, R., van Dijk, A. I. J. M., Beringer, J., Culvenor, D., Evans, B., Huete, A., Hutley, L. B., Maier, S., Restrepo-Coupe, N., Sonnentag, O., Specht, A., Taylor, J. R., van Gorsel, E., and Liddell, M. J.: Australian vegetation phenology: new insights from remote sensing and digital repeat photography *Biogeosciences Discuss.*, doi:10.5194/bg-2016-175, 2016b.
- Mott, J.: Dormancy and Germination in Five Native Grass Species From Savannah Woodland Communities of the Northern Territory, *Australian Journal of Botany*, 26, 621-631, <http://dx.doi.org/10.1071/BT9780621>, 1978.
- Murphy, B. P., Russell-Smith, J., and Prior, L. D.: Frequent fires reduce tree growth in northern Australian savannas: Implications for tree demography and carbon sequestration, *Global Change Biology*, 16, 331-343, 2010.
- Noormets, A.: *Phenology of Ecosystem Processes*, Springer, New York, 2009.
- O'Grady, A. P., Eamus, D., and Hutley, L. B.: Transpiration increases during the dry season: Patterns of tree water use in eucalypt open-forests of northern Australia, *Tree Physiology*, 19, 591-597, 1999.
- O'Grady, A. P., Chen, X., Eamus, D., and Hutley, L. B.: Composition, leaf area index and standing biomass of eucalypt open forests near Darwin in the Northern Territory, Australia, *Australian Journal of Botany*, 48, 629-638, 2000.
- Osborne, C. P., and Beerling, D. J.: Nature's green revolution: The remarkable evolutionary rise of C₄ plants, *Philosophical Transactions of the Royal Society B: Biological Sciences*, 361, 173-194, doi:10.1038/35075035, 2006.
- Prior, L. D., Eamus, D., and Bowman, D. M. J. S.: Tree growth rates in north Australian savanna habitats: Seasonal patterns and correlations with leaf attributes, *Australian Journal of Botany*, 52, 303-314, 2004.
- Ratnam, J., Bond, W. J., Fensham, R. J., Hoffmann, W. A., Archibald, S., Lehmann, C. E. R., Anderson, M. T., Higgins, S. I., and Sankaran, M.: When is a 'forest' a savanna, and why does it matter?, *Global Ecology and Biogeography*, 20, 653-660, 2011.
- Reichstein, M., Falge, E., Baldocchi, D., Papale, D., Aubinet, M., Berbigier, P., Bernhofer, C., Buchmann, N., Gilmanov, T., Granier, A., Grünwald, T., Havránek, K., Ilvesniemi, H., Janous, D., Knohl, A., Laurila, T., Lohila, A., Loustau, D., Matteucci, G., Meyers, T., Miglietta, F., Ourcival, J. M., Pumpanen, J., Rambal, S., Rotenberg, E., Sanz, M., Tenhunen, J., Seufert, G., Vaccari, F., Vesala, T., Yakir, D., and Valentini, R.: On the separation of net ecosystem exchange into assimilation and ecosystem respiration: Review and improved algorithm, *Global Change Biology*, 11, 1424-1439, 2005.
- Reisinger, A., Kitching, R. L., Chiew, F., Hughes, L., Newton, P. C. D., Schuster, S. S., Tait, A., and Whetton, P.: Australasia, in: *Climate Change 2014: Impacts, Adaptation, and Vulnerability. Part B: Regional Aspects. Contribution of Working Group II to the Fifth Assessment Report of the*



Intergovernmental Panel of Climate Change, edited by: Barros, V. R., Field, C. B., Dokken, D. J., Mastrandrea, M. D., Mach, K. J., Bilir, T. E., Chatterjee, M., Ebi, K. L., Estrada, Y. O., Genova, R. C., Girma, B., Kissel, E. S., Levy, A. N., MacCracken, S., Mastrandrea, P. R., and White, L. L., Cambridge University Press, Cambridge, United Kingdom and New York, NY, USA, 1371-1438, 2014.

Restrepo-Coupe, N., Huete, A., Davies, K., Cleverly, J., Beringer, J., Eamus, D., van Gorsel, E., Hutley, L., and Meyer, W. S.: MODIS vegetation products as proxies of photosynthetic potential: a look across meteorological and biologic driven ecosystem productivity, *Biogeosciences Discussions*, 12, 19213-19267, 2015.

Richardson, A. D., Jenkins, J. P., Braswell, B. H., Hollinger, D. Y., Ollinger, S. V., and Smith, M. L.: Use of digital webcam images to track spring green-up in a deciduous broadleaf forest, *Oecologia*, 152, 323-334, 2007.

Richardson, A. D., Braswell, B. H., Hollinger, D. Y., Jenkins, J. P., and Ollinger, S. V.: Near-surface remote sensing of spatial and temporal variation in canopy phenology, *Ecological Applications*, 19, 1417-1428, 2009a.

Richardson, A. D., Hollinger, D. Y., Dail, D. B., Lee, J. T., Munger, J. W., and O'Keefe, J.: Influence of spring phenology on seasonal and annual carbon balance in two contrasting New England forests, *Tree Physiology*, 29, 321-331, 2009b.

Richardson, A. D., Black, T. A., Ciais, P., Delbart, N., Friedl, M. A., Gobron, N., Hollinger, D. Y., Kutsch, W. L., Longdoz, B., Luyssaert, S., Migliavacca, M., Montagnani, L., Munger, J. W., Moors, E., Piao, S., Rebmann, C., Reichstein, M., Saigusa, N., Tomelleri, E., Vargas, R., and Varlagin, A.: Influence of spring and autumn phenological transitions on forest ecosystem productivity, *Philosophical Transactions of the Royal Society B: Biological Sciences*, 365, 3227-3246, 2010.

Richardson, A. D., Keenan, T. F., Migliavacca, M., Ryu, Y., Sonnentag, O., and Toomey, M.: Climate change, phenology, and phenological control of vegetation feedbacks to the climate system, *Agricultural and Forest Meteorology*, 169, 156-173, 2013.

Rogers, C., and Beringer, J.: Describing rainfall in northern Australia using multiple climate indices, *Biogeosciences Discuss.*, 2016, 1-39, 10.5194/bg-2016-172, 2016.

Running, S. W., and Zhao, M.: User's Guide: Daily GPP and annual NPP (MOD17 A2/A3) products, NASA Earth Observing System MODIS land algorithm 1-28, 2015.

Ryu, Y., Sonnentag, O., Nilson, T., Vargas, R., Kobayashi, H., Wenk, R., and Baldocchi, D. D.: How to quantify tree leaf area index in an open savanna ecosystem: A multi-instrument and multi-model approach, *Agricultural and Forest Meteorology*, 150, 63-76, 10.1016/j.agrformet.2009.08.007, 2010.

Ryu, Y., Baldocchi, D. D., Kobayashi, H., Van Ingen, C., Li, J., Black, T. A., Beringer, J., Van Gorsel, E., Knohl, A., Law, B. E., and Rouspard, O.: Integration of MODIS land and atmosphere products with a coupled-process model to estimate gross primary productivity and evapotranspiration from 1 km to global scales, *Global Biogeochemical Cycles*, 25, 2011.

Ryu, Y., Verfaillie, J., Macfarlane, C., Kobayashi, H., Sonnentag, O., Vargas, R., Ma, S., and Baldocchi, D. D.: Continuous observation of tree leaf area index at ecosystem scale using upward-pointing digital cameras, *Remote Sensing of Environment*, 126, 116-125, 10.1016/j.rse.2012.08.027, 2012.

Sage, R. F.: The evolution of C4 photosynthesis, *New Phytologist*, 161, 341-370, 2004.



Savitzky, A., and Golay, M. J. E.: Smoothing and differentiation of data by simplified least squares procedures, *Analytical Chemistry*, 36, 1627-1639, 1964.

Scheiter, S., Higgins, S. I., Beringer, J., and Hutley, L. B.: Climate change and long-term fire management impacts on Australian savannas, *New Phytologist*, 205, 1211-1226, 2015.

Scholes, R. J., and Archer, S. R.: Tree-grass interactions in Savannas, *Annual Review of Ecology and Systematics*, 28, 517-544, 1997.

Scott, K. A., Setterfield, S. A., Douglas, M. M., and Andersen, A. N.: Environmental factors influencing the establishment, height and fecundity of the annual grass *Sorghum intrans* in an Australian tropical savanna, *Journal of Tropical Ecology*, 26, 313-322, 2010.

Sjöström, M., Zhao, M., Archibald, S., Arneth, A., Cappelaere, B., Falk, U., de Grandcourt, A., Hanan, N., Kergoat, L., Kutsch, W., Merbold, L., Mougin, E., Nickless, A., Nouvellon, Y., Scholes, R. J., Veenendaal, E. M., and Ardö, J.: Evaluation of MODIS gross primary productivity for Africa using eddy covariance data, *Remote Sensing of Environment*, 131, 275-286, 10.1016/j.rse.2012.12.023, 2013.

Sonnentag, O., Hufkens, K., Teshera-Sterne, C., Young, A. M., Friedl, M., Braswell, B. H., Milliman, T., O'Keefe, J., and Richardson, A. D.: Digital repeat photography for phenological research in forest ecosystems, *Agricultural and Forest Meteorology*, 152, 159-177, 2012.

Specht, R. L.: Vegetation, in: *Australian Environment*, 4 ed., edited by: Leeper, G. W., Melbourne University Press, Melbourne, 44-67, 1972.

Tagesson, T., Fensholt, R., Cropley, F., Guiro, I., Horion, S., Ehammer, A., and Ardö, J.: Dynamics in carbon exchange fluxes for a grazed semi-arid savanna ecosystem in West Africa, *Agriculture, Ecosystems and Environment*, 205, 15-24, 10.1016/j.agee.2015.02.017, 2015.

Tans, P. P., Fung, I. Y., and Takahashi, T.: Observational constraints on the global atmospheric CO₂ budget, *Science*, 247, 1431-1438, 1990.

Toomey, M., Friedl, M. A., Froliking, S., Hufkens, K., Klosterman, S., Sonnentag, O., Baldocchi, D. D., Bernacchi, C. J., Biraud, S. C., Bohrer, G., Brzostek, E., Burns, S. P., Coursolle, C., Hollinger, D. Y., Margolis, H. A., McCaughey, H., Monson, R. K., Munger, J. W., Pallardy, S., Phillips, R. P., Torn, M. S., Wharton, S., Zeri, M., and Richardson, A. D.: Greenness indices from digital cameras predict the timing and seasonal dynamics of canopy-scale photosynthesis, *Ecological Applications*, 25, 99-115, 2015.

Tucker, C. J.: Red and photographic infrared linear combinations for monitoring vegetation, *Remote Sensing of Environment*, 8, 127-150, 1979.

van Gorsel, E., Delpierre, N., Leuning, R., Black, A., Munger, J. W., Wofsy, S., Aubinet, M., Feigenwinter, C., Beringer, J., Bonal, D., Chen, B., Chen, J., Clement, R., Davis, K. J., Desai, A. R., Dragoni, D., Etzold, S., Grünwald, T., Gu, L., Heinesch, B., Huttyra, L. R., Jans, W. W. P., Kutsch, W., Law, B. E., Leclerc, M. Y., Mammarella, I., Montagnani, L., Noormets, A., Rebmann, C., and Wharton, S.: Estimating nocturnal ecosystem respiration from the vertical turbulent flux and change in storage of CO₂, *Agricultural and Forest Meteorology*, 149, 1919-1930, 2009.

Van Langevelde, F., Van De Vijver, C. A. D. M., Kumar, L., Van De Koppel, J., De Ridder, N., Van Andel, J., Skidmore, A. K., Hearne, J. W., Stroosnijder, L., Bond, W. J., Prins, H. H. T., and Rietkerk, M.: Effects of fire and herbivory on the stability of savanna ecosystems, *Ecology*, 84, 337-350, 2003.



- Weiss, M., Baret, F., Smith, G. J., Jonckheere, I., and Coppin, P.: Review of methods for in situ leaf area index (LAI) determination Part II. Estimation of LAI, errors and sampling, *Agricultural and Forest Meteorology*, 121, 37-53, 2004.
- Werner, P. A., and Franklin, D. C.: Resprouting and mortality of juvenile eucalypts in an Australian savanna: Impacts of fire season and annual sorghum, *Australian Journal of Botany*, 58, 619-628, 2010.
- Werner, P. A., and Prior, L. D.: Demography and growth of subadult savanna trees: Interactions of life history, size, fire season, and grassy understory, *Ecological Monographs*, 83, 67-93, 2013.
- Whitley, R. J., Macinnis-Ng, C. M. O., Hutley, L. B., Beringer, J., Zeppel, M., Williams, M., Taylor, D., and Eamus, D.: Is productivity of mesic savannas light limited or water limited? Results of a simulation study, *Global Change Biology*, 17, 3130-3149, 2011.
- Williams, R. J., Myers, B. A., Muller, W. J., Duff, G. A., and Eamus, D.: Leaf phenology of woody species in a North Australian tropical savanna, *Ecology*, 78, 2542-2558, 1997.
- Woebbecke, D. M., Meyer, G. E., Von Bargen, K., and Mortensen, D. A.: Color indices for weed identification under various soil, residue, and lighting conditions, *Transactions of the American Society of Agricultural Engineers*, 38, 259-269, 1995.
- Wu, J., Albert, L. P., Lopes, A. P., Restrepo-Coupe, N., Hayek, M., Wiedemann, K. T., Guan, K., Stark, S. C., Christoffersen, B., Prohaska, N., Tavares, J. V., Marostica, S., Kobayashi, H., Ferreira, M. L., Campos, K. S., da Silva, R., Brando, P. M., Dye, D. G., Huxman, T. E., Huete, A., Nelson, B. W., and Saleska, S. R.: Leaf development and demography explain photosynthetic seasonality in Amazon evergreen forests, *Science*, 351, 972-976, 2016.
- Yan, H., Wang, S. Q., Billesbach, D., Oechel, W., Bohrer, G., Meyers, T., Martin, T. A., Matamala, R., Phillips, R. P., Rahman, F., Yu, Q., and Shugart, H. H.: Improved global simulations of gross primary product based on a new definition of water stress factor and a separate treatment of C3 and C4 plants, *Ecological Modelling*, 297, 42-59, 10.1016/j.ecolmodel.2014.11.002, 2015.
- Yuan, W., Liu, S., Zhou, G., Zhou, G., Tieszen, L. L., Baldocchi, D., Bernhofer, C., Gholz, H., Goldstein, A. H., Goulden, M. L., Hollinger, D. Y., Hu, Y., Law, B. E., Stoy, P. C., Vesala, T., and Wofsy, S. C.: Deriving a light use efficiency model from eddy covariance flux data for predicting daily gross primary production across biomes, *Agricultural and Forest Meteorology*, 143, 189-207, 10.1016/j.agrformet.2006.12.001, 2007.
- Zhao, M., and Running, S. W.: Drought-induced reduction in global terrestrial net primary production from 2000 through 2009, *Science*, 329, 940-943, 10.1126/science.1192666, 2010.
- Zhu, X. G., Long, S. P., and Ort, D. R.: What is the maximum efficiency with which photosynthesis can convert solar energy into biomass?, *Current Opinion in Biotechnology*, 19, 153-159, 10.1016/j.copbio.2008.02.004, 2008.



Table 1: Understory biomass harvest information for Howard Springs savanna collected across the wet seasons from 2012 to 2014.

Period	Grass biomass (t ha ⁻¹)	Other biomass (t ha ⁻¹)	Grass biomass (%)	Other biomass (%)
Start Wet – Dec	0.46	0.96	33	67
Mid Wet – Feb	1.34	1.77	43	57
Peak Wet – Mar	1.55	1.09	59	41
End Wet - Apr	1.31	0.38	77	23



Table 2: Summary of model performances against flux tower estimated GPP for overstory and understory at Howard Springs. Statistics include the Pearson Correlation coefficient (Corr), the root mean square error (RMSE, $\text{g C m}^{-2} \text{d}^{-1}$) and the relative predictive error (RPE, %) for the light use efficiency model (LUE), LUE with evaporative fraction (LUE_EF), LUE with green chromatic coordinates (LUE_GCC) and LUE with EF and GCC (LUE_EF_GCC). The * highlights that the MODIS enhanced vegetation index (EVI) is used instead of GCC for the Ecosystem analysis. Pearson p values are not included as all were significant with $P < 0.001$.

	Model	Overstory				Understory				Ecosystem*			
		Corr	RMSE	RPE		Corr	RMSE	RPE		Corr	RMSE	RPE	
All years	LUE	0.64	1.45	-1.79		0.57	2.02	62.09		0.80	2.11	13.77	
	LUE_EF	0.73	1.47	8.40		0.73	1.43	22.27		0.79	2.69	25.18	
	LUE_GCC/EVI*	0.60	1.43	-0.85		0.78	1.40	55.32		0.81	2.09	14.85	
	LUE_EF_GCC/EVI*	0.72	1.36	8.44		0.85	0.96	17.73		0.83	2.48	25.51	
Wet Season (15 Oct - 15 Apr)	LUE	0.61	1.59	13.30		0.33	2.28	30.89		0.72	2.42	15.53	
	LUE_EF	0.68	1.85	22.76		0.43	1.92	21.60		0.66	3.18	25.26	
	LUE_GCC/EVI*	0.61	1.50	14.02		0.59	1.43	26.95		0.74	2.42	18.92	
	LUE_EF_GCC/EVI*	0.70	1.67	23.13		0.66	1.25	19.33		0.71	3.07	28.36	
Dry Season (16 Apr - 14 Oct)	LUE	0.37	1.32	-17.97		0.54	1.76	159.34		0.56	1.80	11.21	
	LUE_EF	0.63	1.05	-7.76		0.48	0.84	24.36		0.71	2.19	25.06	
	LUE_GCC/EVI*	0.24	1.37	-16.80		0.41	1.38	143.73		0.39	1.76	8.94	
	LUE_EF_GCC/EVI*	0.57	1.03	-7.31		0.32	0.62	12.73		0.63	1.84	21.38	

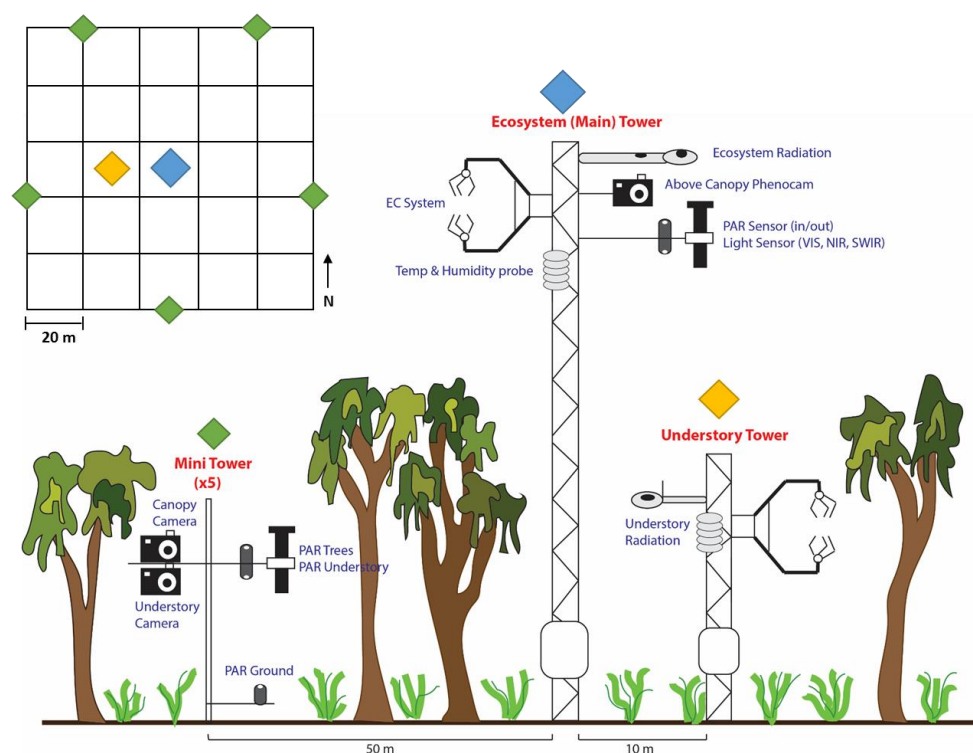


Figure 1: Diagram showing the core instrumentation supported by each flux tower and mini tower at the Howard Springs OzFlux site, as well as the layout of the monitoring plot.

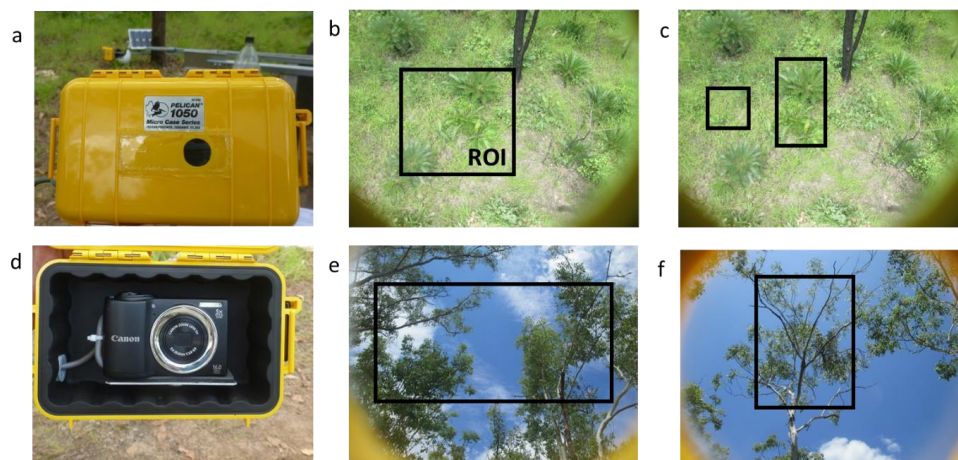


Figure 2: Camera setup (a & d) and examples of understory (b & c) and overstory (e & f) regions of interest (ROI, black box) used from phenocam images collected at the Howard Springs OzFlux site.

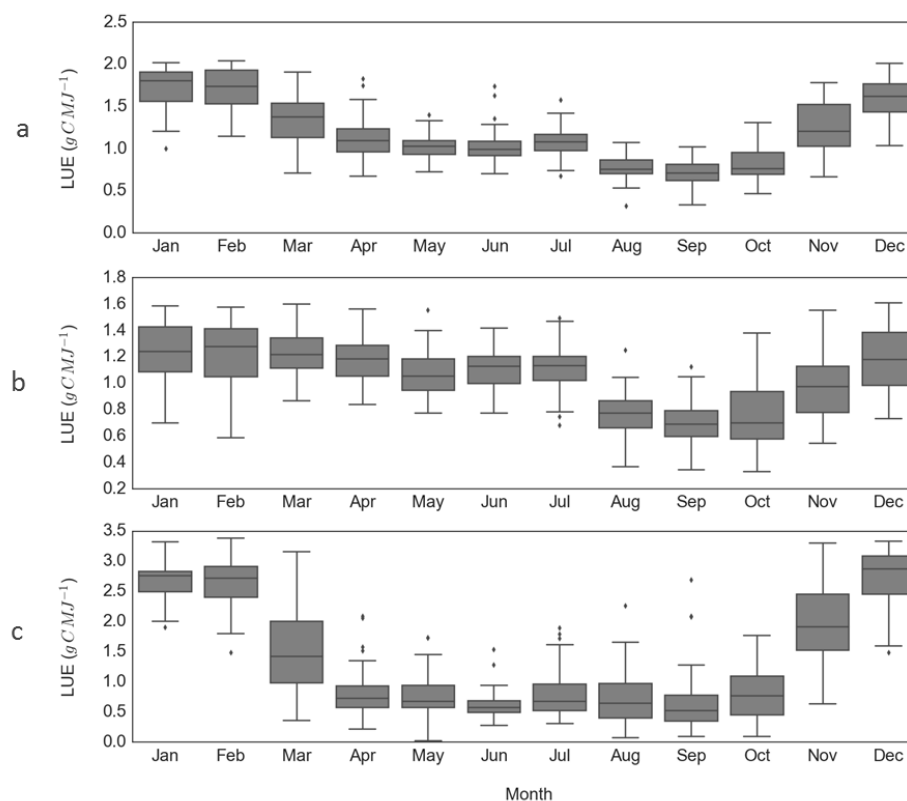


Figure 3: Monthly mean light use efficiency (LUE) \pm SE (boxes) with 95 % confidence (whiskers) for the Howard Springs OzFlux site ecosystem (a), overstory (b) and understory (c) from December 2012 to October 2014. Individual dots represent outlier values for each respective month.

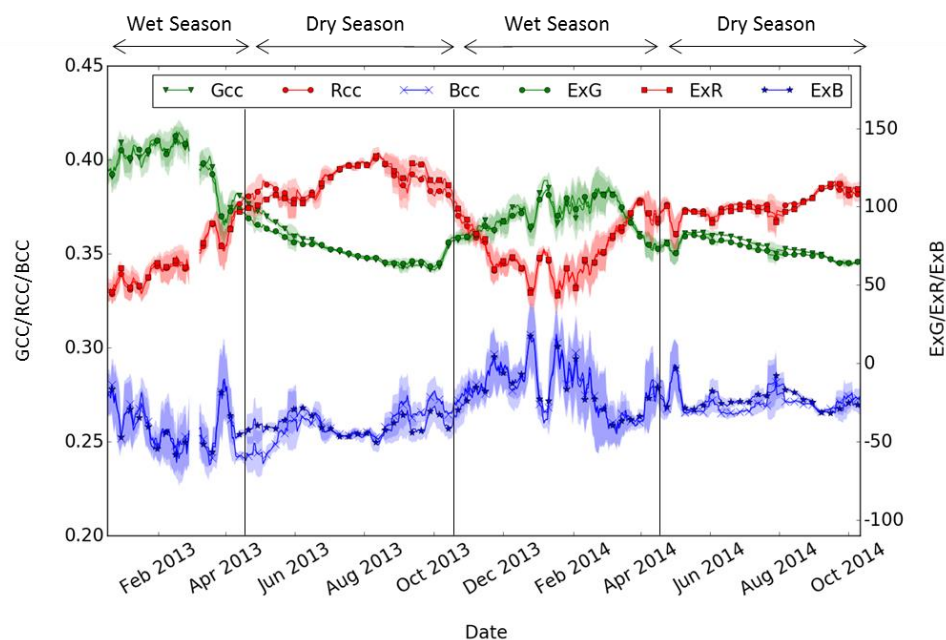


Figure 4: Daily green, red and blue chromatic coordinates (GCC/RCC/BCC) and excess indices (ExG/ExR/ExB) for the Howard Springs OzFlux site understory from December 2012 to October 2014. Daily data are shown with an 8-day centred running mean (marked every 8 days for visualisation) applied. The standard error of the mean is given by the shading.

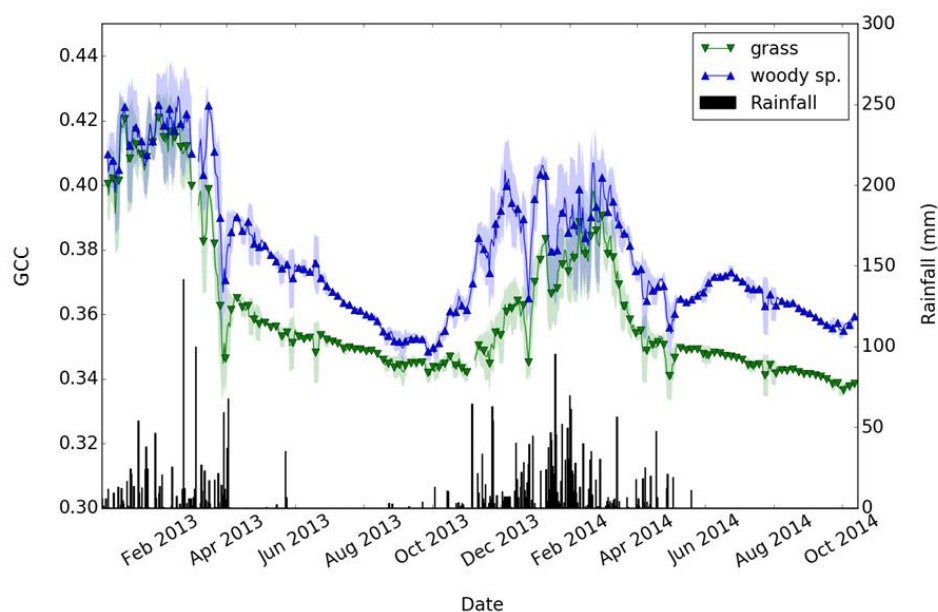


Figure 5: Daily rainfall (mm) and green chromatic coordinate (GCC) time series for grass and other woody green species (woody sp.) found in the savanna understory at the Howard Springs OzFlux site from December 2012 to October 2014. The GCC daily data are shown with an 8-day centred running mean (marked every 8 days for visualisation) applied. The standard error of the mean is given by the shading. The GCC time series represent the change in relative greenness of grass and woody species, not the absolute sum of grass versus woody species biomass in the understory.

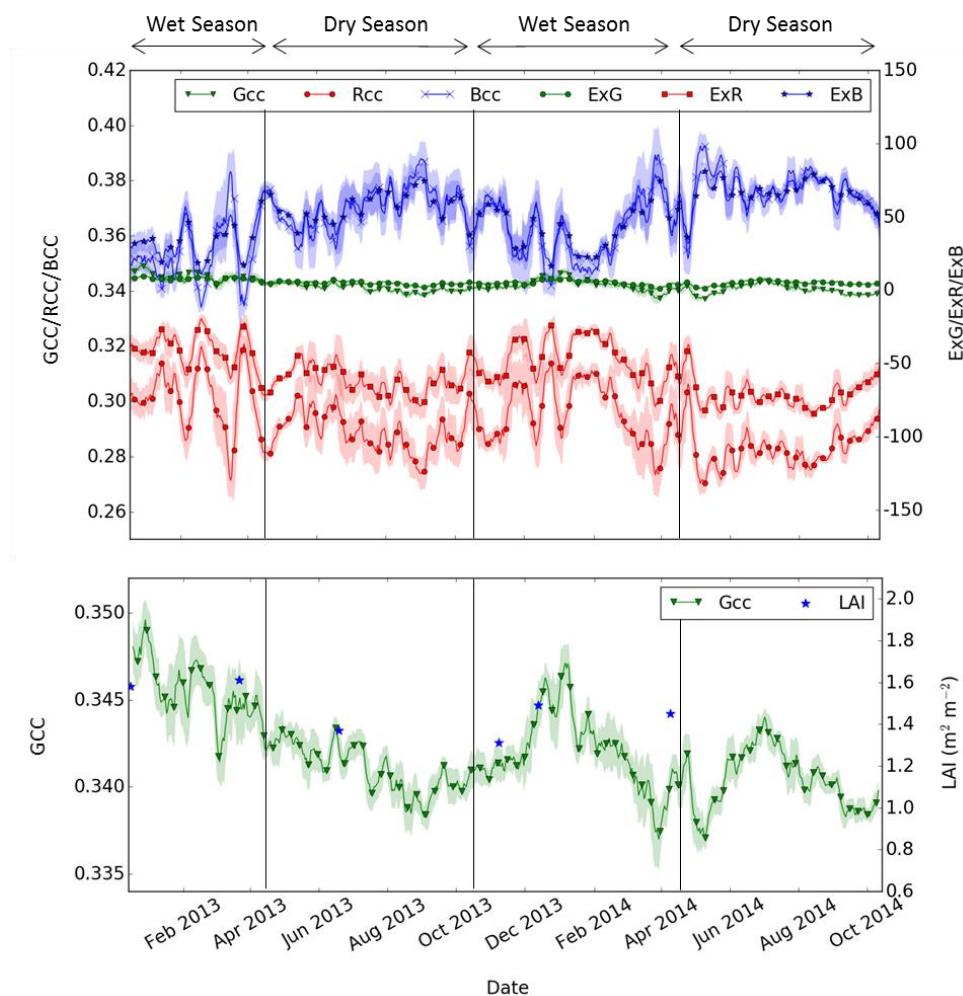


Figure 6: Daily green, red and blue chromatic coordinates (GCC/RCC/BCC) and excess indices (ExG/ExR/ExB) for the Howard Springs OzFlux site overstory (a), plus GCC and leaf area index (LAI) for the overstory (b) from December 2012 to October 2014. Daily data are shown with an 8-day centred running mean (marked every 8 days for visualisation) applied. The standard error of the mean is given by the shading.

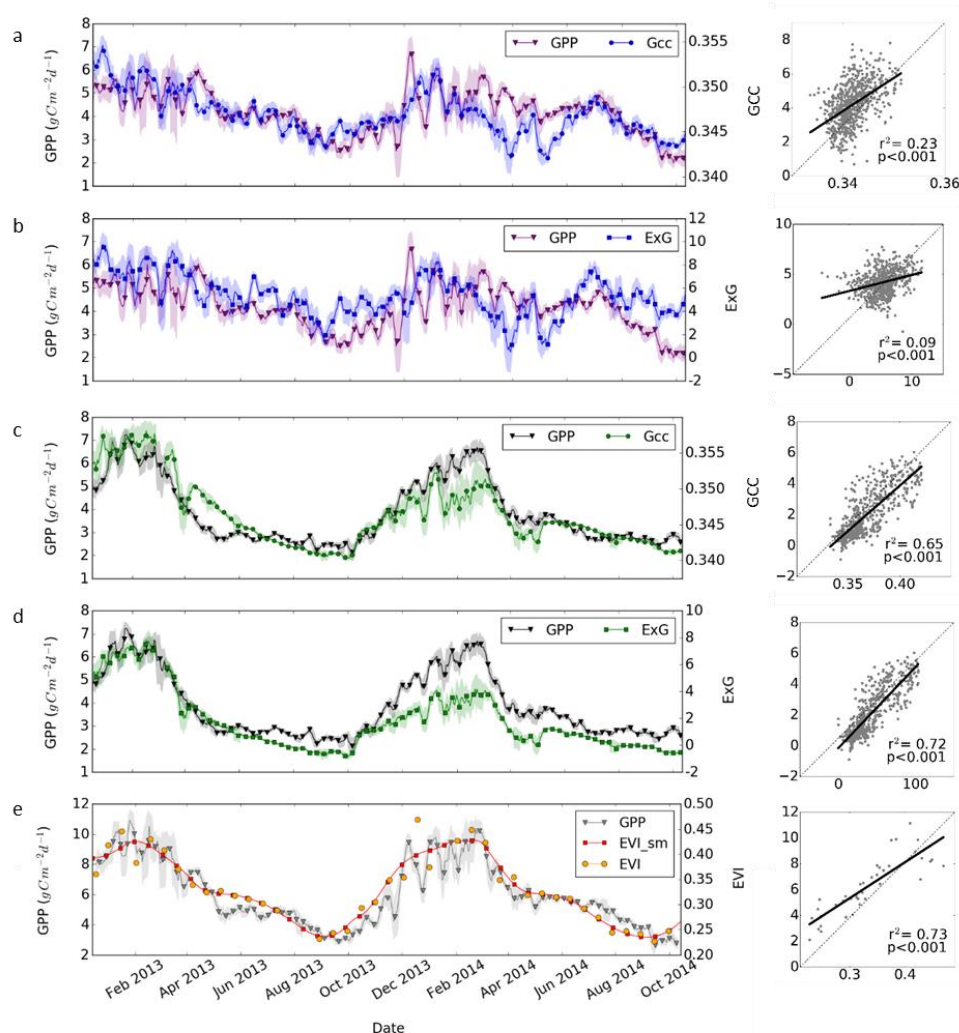


Figure 7: Overstory (a & b) and understory (c & d) flux tower GPP with green chromatic coordinate (GCC) and excess green (ExG) indices, as well as ecosystem flux tower GPP with MODIS enhanced vegetation index (EVI, e), from December 2012 to October 2014 at the Howard Springs OzFlux site. Daily data are shown with an 8-day running mean (marked every 8 days for visualisation) applied. The standard error of the mean is given by the shading. Included for each time series are the respective regression plots showing r^2 and p values for GCC/ExG/EVI (x) against flux tower GPP (y). For MODIS EVI (e) the time series plot includes raw 16 day values (EVI) and a Savitzky-Golay smoothed daily EVI product (EVI_sm), with the regression plot showing the raw 16 day EVI and the corresponding GPP for that day.

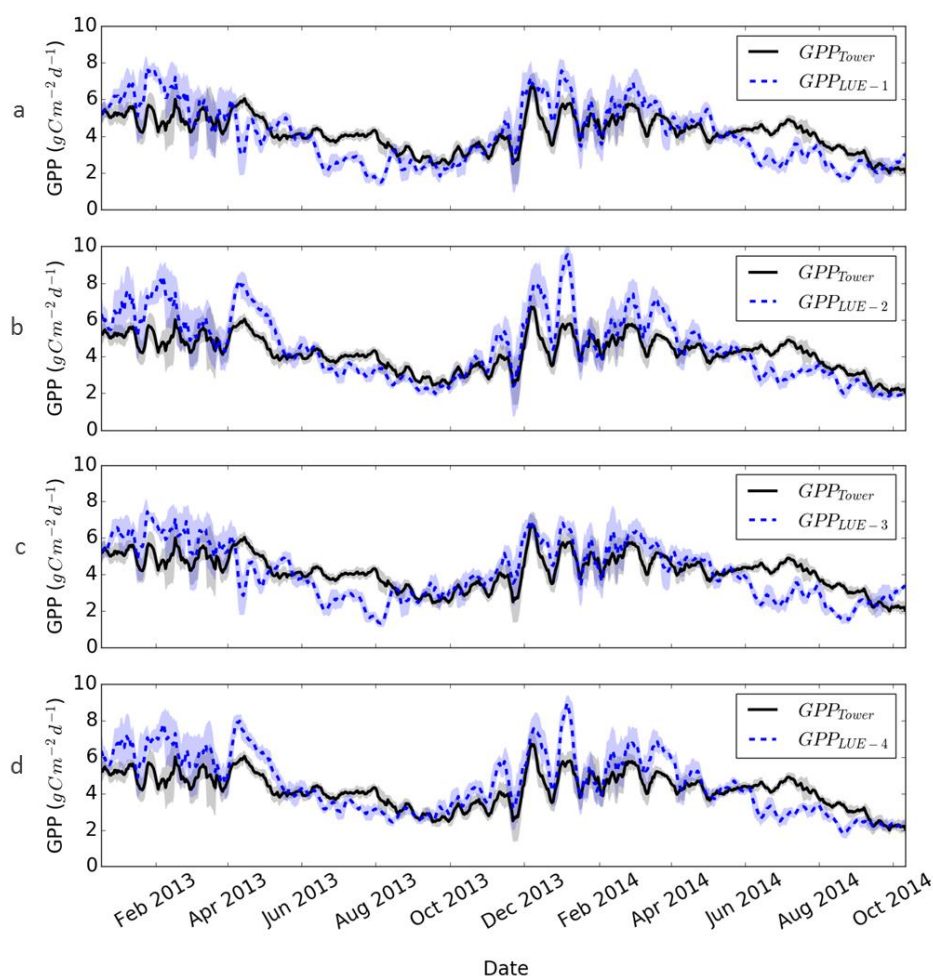


Figure 8: Overstory flux tower estimated GPP with model predicted GPP for the Howard Springs OzFlux site. Models shown are a) light use efficiency (LUE-1), b) LUE with evaporative fraction (LUE-2), c) LUE with green chromatic coordinates (LUE-3), d) and LUE with EF and GCC (LUE-4).

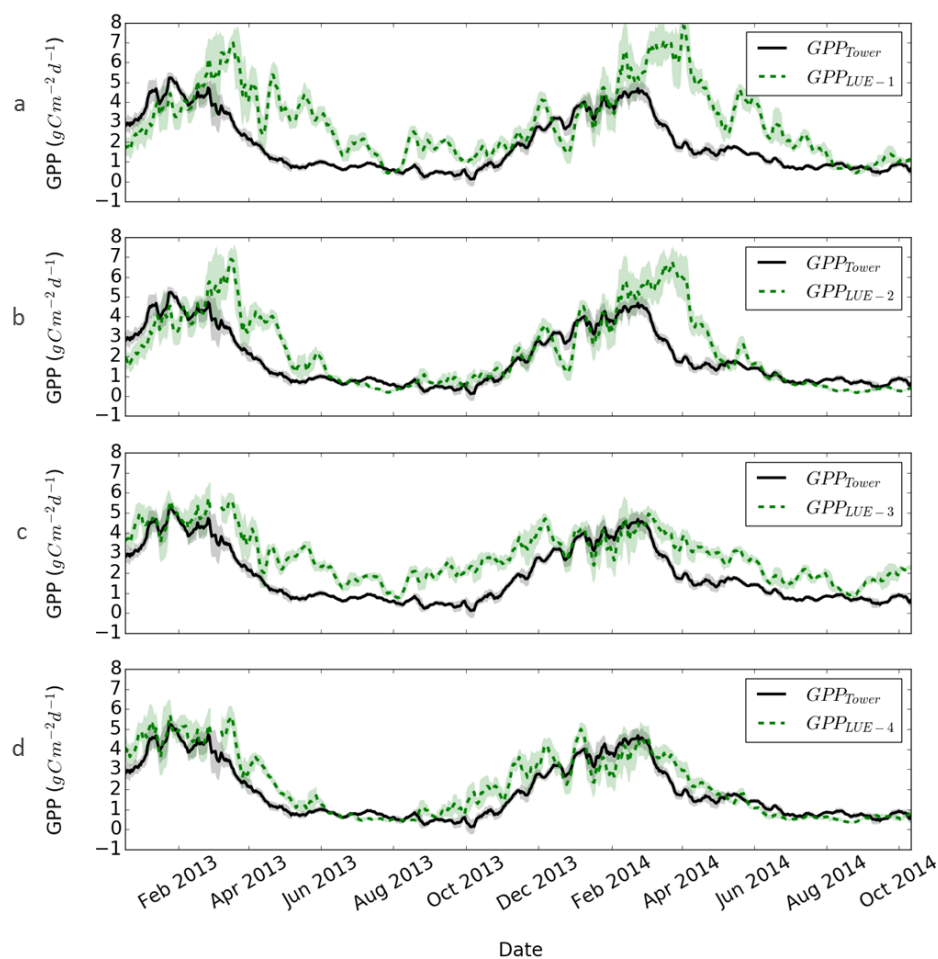


Figure 9: Understory flux tower estimated GPP with model predicted GPP for the Howard Springs OzFlux site. Models shown are a) light use efficiency (LUE-1), b) LUE with evaporative fraction (LUE-2), c) LUE with green chromatic coordinates (LUE-3), d) and LUE with EF and GCC (LUE-4).

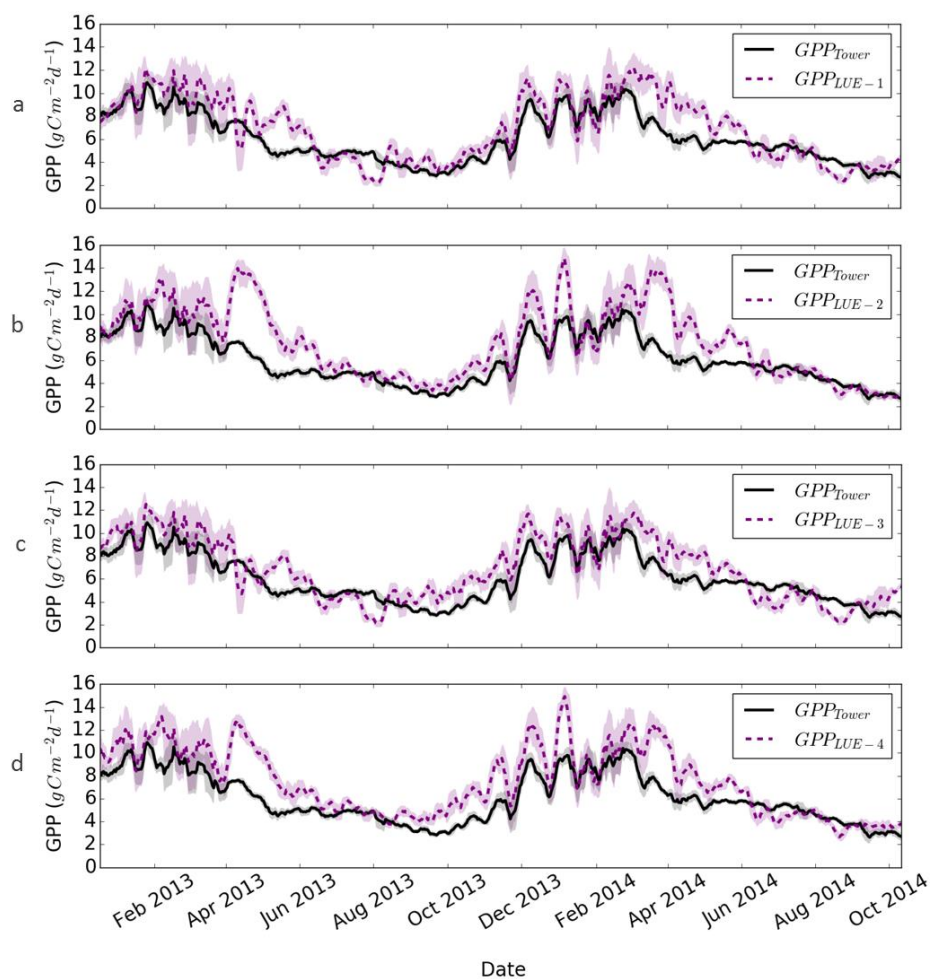


Figure 10: Ecosystem flux tower estimated GPP with model predicted GPP for the Howard Springs OzFlux site. Models shown are a) light use efficiency (LUE-1), b) LUE with evaporative fraction (EF, LUE-2), c) LUE with MODIS enhanced vegetation index (EVI, LUE-3), d) and LUE with EF and EVI (LUE-4).